Copyright Warning & Restrictions

The copyright law of the United States (Title 17, United States Code) governs the making of photocopies or other reproductions of copyrighted material.

Under certain conditions specified in the law, libraries and archives are authorized to furnish a photocopy or other reproduction. One of these specified conditions is that the photocopy or reproduction is not to be "used for any purpose other than private study, scholarship, or research." If a, user makes a request for, or later uses, a photocopy or reproduction for purposes in excess of "fair use" that user may be liable for copyright infringement,

This institution reserves the right to refuse to accept a copying order if, in its judgment, fulfillment of the order would involve violation of copyright law.

Please Note: The author retains the copyright while the New Jersey Institute of Technology reserves the right to distribute this thesis or dissertation

Printing note: If you do not wish to print this page, then select "Pages from: first page # to: last page #" on the print dialog screen

THE EFFECT OF VELOCITY
ON THE ELECTRICAL CONDUCTIVITY OF BLOOD

BY

JUDEA PEARL

A THESIS

PRESENTED IN PARTIAL FULFILLMENT OF

THE REQUIREMENTS FOR THE DEGREE

OF

MASTER OF SCIENCE IN ELECTRICAL ENGINEERING

AT

NEWARK COLLEGE OF ENGINEERING

Newark, New Jersey
1961

APPROVAL OF THESIS

FOR

DEPARTMENT OF ELECTRICAL ENGINEERING

NEWARK COLLEGE OF ENGINEERING

BY

FACULTY COMMITTEE

APPROVED: _____

_____

_____

NEWARK, NEW JERSEY

JUNE, 1961

ABSTRACT

Although the change in the conductance of blood resulting from changes in its velocity has been noted by several investigators working with electrical impedance techniques, this parameter of measurement has heretofore not been investigated from the viewpoint of practical application to blood flow measurement.

In certain regions of the body such as the tooth pulp and the cranial cavity, the volume of the contained blood cannot fluctuate during a cardiac cycle because of the rigid wall of the chamber. Therefore, impedance pulses which have been obtained in studies on the tooth pulp, must be attributed to the rhythmical fluctuation of the conductance of the blood resulting from changes in its velocity.

The scope of this paper is concerned with a theoretical analysis of several factors accounting for the above phenomenon and comparison of the theoretical results with experimental data obtained for different types of circulatory models.

ACKNOWLEDGEMENT

The experimental work on which this thesis is based was conducted in the Murry and Leonie Guggenheim Foundation Institute for Dental Research and the Department of Physiology and Pharmacology at New York University College of Dentistry. Permission to use this aspect of the project for thesis credit was granted by Dr. Frederick M. Liebman, Assistant Professor of Physiology and Pharmacology at the College of Dentistry and Research Associate at the Guggenheim Institute.

I am indebted to Dr. Frederick M. Liebman for his guidance and understanding in outlining the problem, and for his invaluable assistance in sharing both his knowledge and experience.

I also wish to express my appreciation to Mr. Stephen E. Scrupski of Newark College of Engineering for his advisory help in the preparation of this paper.

PREFACE

There are several lines of evidence to support the idea that the change in conductance of blood as a function of its velocity is due to alterations in the cross-sectional arrangement of the red blood cells in a blood vessel or tube. The alterations which occur due to velocity are:

1) Axial accumulation of the cells.
2) A uniform orientation of the cells in relation to the vorticity lines.

The changes both in the orientation of the red blood cells, and in their patterns of distribution occur simultaneously, but will be discussed separately in this paper for the sake of simplicity.

In chapter I the red blood cells will be regarded as perfect spheres, and the longitudinal conductance will be calculated as a function of the density distribution alone. The shape of the density distribution function for several rates of flow (the hematocrit profile) will be calculated using the viscosity profile which can be derived from the blood flow-pressure curves.

In chapter II the problem of a preferred orientation of flowing blood cells will be discussed and an experiment will be described which proved the existence of such orientation and some of its characteristics. The change in conductivity due to change in angular position of the cells will be computed using data obtained from a model representing the blood cell and its environment.

The maximum impedance change predicted on the basis of cell accumulation is 6.58%, whereas that predicted on the basis of cell orientation is 5.47%. A total maximum change of about 12% is therefore expected which is close to the experimental results of more than 10% in a steady flow.

The techniques used in the experimental measurements are described in chapter III. The results obtained with steady flow are compared with those predicted on a theoretical basis. However, most of the experiments were done with pulsatile blood flow which approximates more closely the in vivo conditions. The results differ from those obtained with steady flow, but because of the inability to handle the time parameter mathematically pulsatile flow is not included in the analysis.

TABLE OF CONTENTS

LIST OF FIGURES

Page No.

LIST OF TABLES

CHAPTER I

THE EFFECT OF AXIAL ACCUMULATION OF CELLS ON THE CONDUCTIVITY OF BLOOD.

Introduction.

In order to study the density distribution of the cells in flowing blood, we must first consider the behavior of blood as a total fluid. It is not feasible to examine the behavior of an individual moving cell, or the population changes in different parts of the blood vessel, especially in capillary tubes. We shall therefore analyze the experimental results concerning the macrorheological phenomena of blood in order to obtain information about the microrheological behavior in each part of the vascular cross section.

The pressure-flow curves of human blood flowing in glass tubes, for a wide range of radii and hematocrits [1, 2], produce several families of curves, each family being a set of pressure-flow curves over the hematocrit range for a tube of given radius. Fig. I shows a typical set for a tube radius of 183 microns which corresponds in size to a small artery or arteriole (Fig. I.).

The curves are linear at moderate pressure gradients, and bend in toward the origin at very low pressures. The curvature of the lines at the low range of the pressure gradient is an indication of a non-Newtonian property of blood. If for a Newtonian fluid we assume a constant coefficient of viscosity (μ) connecting the gradient of velocity ($\frac{dv}{dr}$) with the tangential component of the stress tensor (t_{zr}).

---

* Hematocrit is defined as the volume ratio of the red cells to the total fluid.

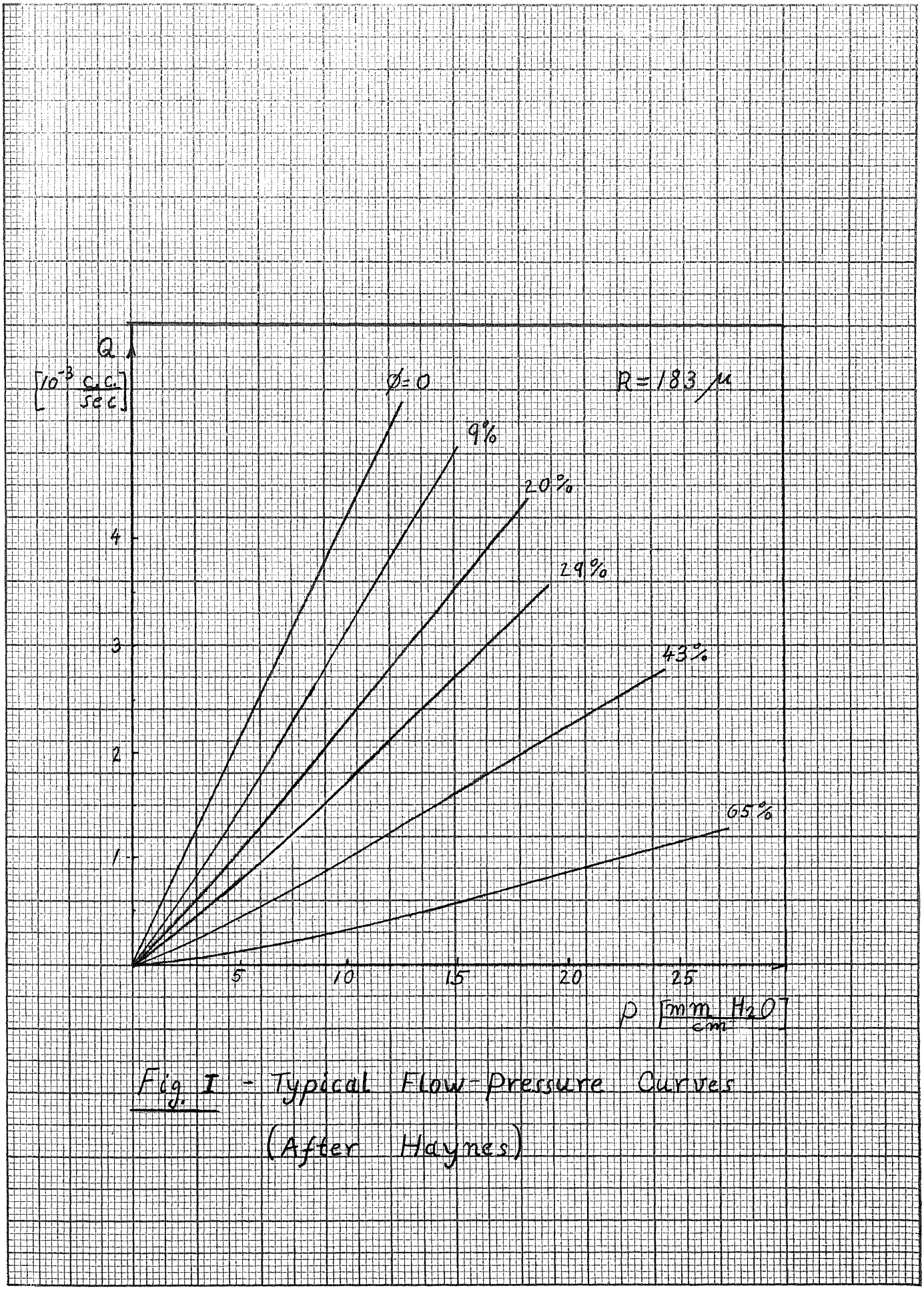

Fig. I - Typical Flow-Pressure Curves
(After Haynes)

$$(1) \quad t_{zr} = \mu \frac{dv}{dr}$$

where t_{zr} is the stress across a plane perpendicular to r, and in the z direction. The z axis is coincident with the axis of the tube, and the velocity (v) is parallel to z at all points, and a function only of the distance (r) from the axis. Then in the equilibrium condition for steady laminar flow the resultant of the tangential stress acting on the boundary surface of each cylindrical lamina and the driving inertial force is zero. $t_{zr} \cdot 2\pi r + \pi r^2 p = 0$

$$(2) \quad t_{zr} = \mu \frac{dv}{dr} = -\frac{Pr}{2}$$

where r is the radius of the observed lamina, v is the velocity in the z direction and P is the pressure gradient per unit length of tube.

The velocity gradient $\frac{dv}{dr}$ becomes linear with r, and vanishes at the center of the tube.

The velocity profile can be easily found by integration, with the boundary condition: $v(R) = 0$

$$(3) \quad V(r) = \int_R^r \frac{dv}{dr}\, dr = -\int_R^r \frac{P}{2} \frac{r}{\mu}\, dr = \frac{P}{4\mu}(R^2 - r^2)$$

The total flow Q (cm^3/sec) is:

$$(4) \quad Q = \int_0^R v(r)\, 2\pi r\, dr = \frac{\pi}{8} \frac{R^4}{\mu} P$$

For a Newtonian fluid the flow-pressure graphs are straight lines, passing through the origin, and having the slope:

$$\frac{Q}{P} = \frac{\pi R^4}{8\mu}$$

The viscosity coefficient μ is expressed as:

$$(5)\quad \mu = \frac{\pi}{8} R^4 \frac{P}{Q}$$

If we compute from the experimental flow-pressure curves (Fig. I) the quantity $\frac{R^4 P}{8 Q}$ and plot it against the pressure, we shall not get a constant, but a curve similar to that of Fig. II.

Applied to a non-Newtonian fluid the quantity $\pi \frac{R^4 P}{8 Q}$ is called the apparent viscosity and represents the equivalent Newtonian viscosity which the blood would have to have in order to obtain the same rate of flow under the same conditions. Obviously, the apparent viscosity of blood is not constant, it has its maximum value at low pressure, and asymptotically reaches a final value at a higher level of pressure. We shall denote the asymptotic value of the viscosity by μ_∞.

The above phenomena can be explained by the formation of a "marginal zone" of fluid, free of particles, surrounding an "axial stream" of cells. This distribution is the result of a transverse pressure acting on the cells and forcing them to move toward the center of the tube. The alteration results in a decrease of the net viscosity. Axial accumulation increases the fluidity in those regions of the tube where the rate of shear is greatest, and reduces the fluidity near the axis of the tube where the rate of shear is close to zero. The net effect is an increase in fluidity, and so the viscosity of the blood is decreased as the pressure is increased.

Several factors are involved in the explanation of this phenomenon. Rivlin[3] has shown that if the pressure-flow curves of a fluid

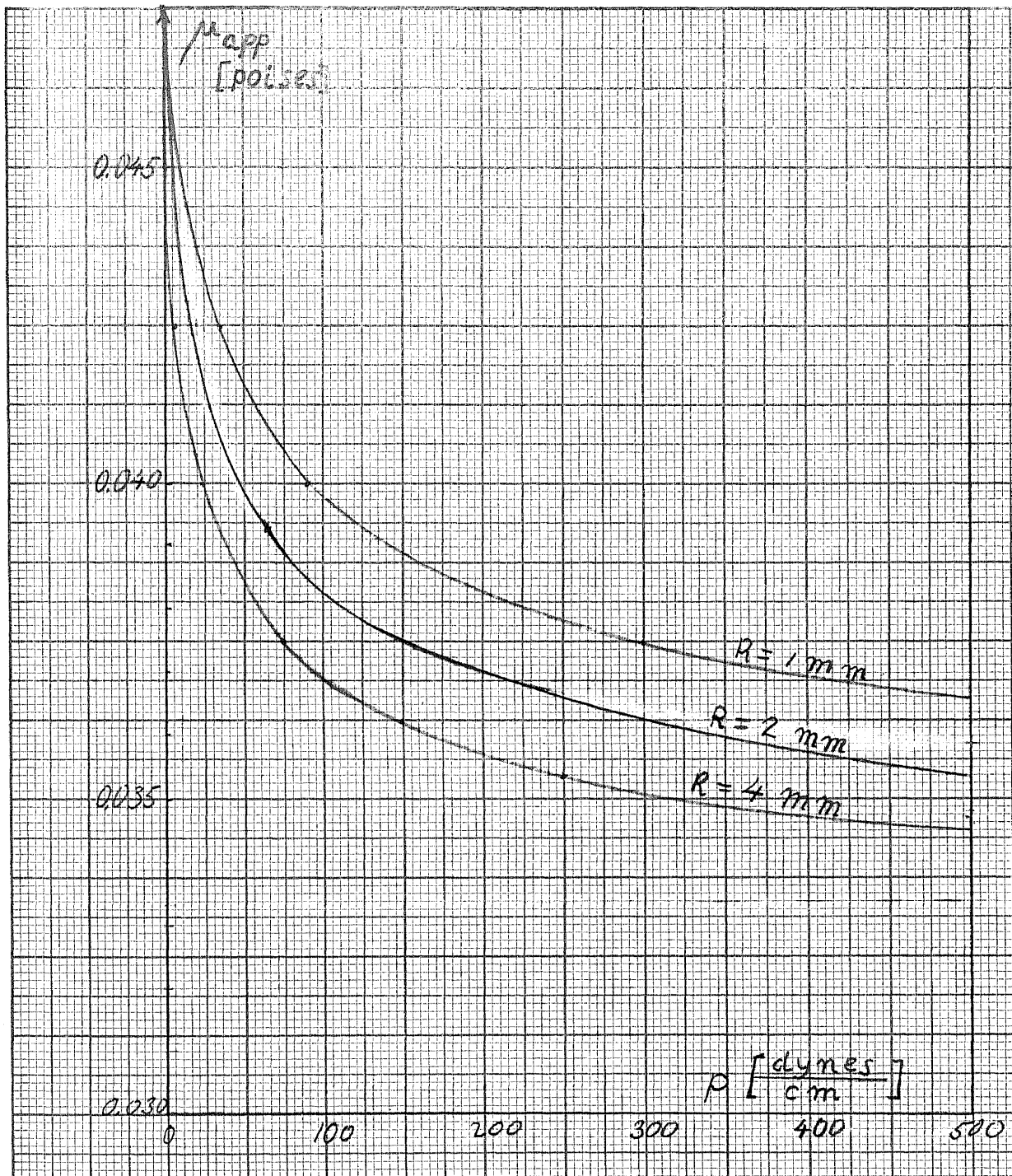

Fig. II - Typical viscosity-pressure curves (After Kümin)

are non-linear, the normal component of the stress tensor does not vanish. In the case of blood, which may be considered as a suspension of small discs, the non-vanishing of the normal components of the stress tensor is reflected in the existence of a transverse force which causes the red cells to accumulate near the axis of the tube. The existence of this force can be explained in terms of the Magnus effect. The velocity on the axial side of the cell is greater that the velocity on the peripheral side (Fig. III). Applying Bernoulli's theorem to streamlines on the axial and peripheral sides of the cell, the existence of the radial drift force becomes apparent.

The difference in velocity also results in a couple, causing the cell to rotate around its axis. The couple plays a great part in the orientation of the cells which will subsequently be discussed in more detail. G. B. Jeffery[4], in his fundamental article on motion of small ellipsoids in a viscous fluid, stated the following hypothesis:

"Particles immersed in a viscous fluid, will tend to adopt that motion which, of all the motions possible, corresponds to the least dissipation of energy."

The viscous energy dissipation associated with each particle depends upon the rate of shear in its environment. Each particle will tend to move from a place where the shear is high to a place where the shear is low, which means, from the periphery to the center of the tube.

The motion of the particles toward the center is limited by other forces tending to disperse them. The most important among them is the "diffusion pressure". As a result of random mutual collisions of

Fig. III

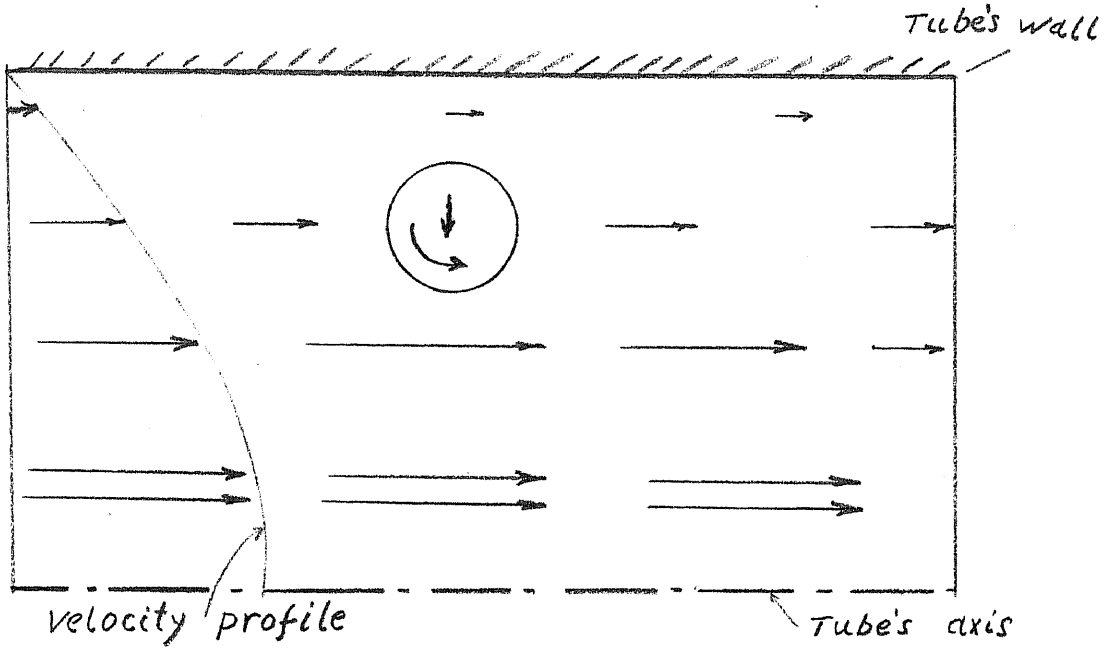

The velocity field results in centripetal force and rotational couple acting on a red cell

the cells, they will tend to move from a dense to a dispersed environment. Other forces which would tend to disperse the particles, are Brownian movement and electrical forces. However, both are too small to have any significant effect, the first because of the relatively large dimensions of the red cell, and the second because of the high ionic concentration of the medium.

Moreover, this effect becomes saturated at finite pressures, and so there is a limit to the increase in fluidity as the pressure is increased. The slope of the pressure-flow curves bends upward, as shown in Fig. I., and the curves become linear when the apparent fluidity reaches its maximum possible value.

By means of a mathematical analysis we shall calculate the viscosity profile and the hematocrit profile across the tube, as a function of the pressure and the diameter of the tube. Knowing the density distribution, we shall be able to compute the resultant electrical conductance.

The assumptions made in the following argument are:

a) Axial accumulation contributes the major share of the non-Newtonian behavior, and so the viscosity is a function only of the volume concentration (or the rate of shear).

b) Axial accumulation gives rise to the major share of the electrical impedance changes. The contribution of the orientation effect to changes in electrical impedance will be discussed separately.

1. The Viscosity Profile.

Algebraic representation of the flow-pressure curves. Many workers tried to use a polynomial to represent the observed data, but this representation is not suitable because the fluidity does not increase indefinitely. This becomes evident by examination of the curves which become linear at higher pressures.

Haynes[2] used an exponential representation:

$$(6)\quad Q = M(R.\phi).P - B(R)\left[1 - e^{-K(R,\phi)P}\right]$$

where Q is the volume rate of flow, P the pressure gradient.

The parameters M, B, and K depend on the tube radius, R, and the hematocrit ϕ. This representation is fairly close to the observed data, but has the disadvantage of not being universal, and including too many undetermined parameters. However, Taylor[5] used the following expression:

$$\mu_{app} = \mu_{\infty}\left(1 + K|S|^{-\frac{1}{2}}\right)$$

where $S = \frac{1}{2}PR$ is the applied wall stress, μ_{∞} is the apparent viscosity at high speeds.

This representation has the advantage of being universal; if the apparent viscosity is plotted against PR, we get one curve for different radii. Examining the data of Kumin[1], K remains almost constant over the range R = 2.5 mm to R = 0.2 mm. This emphasizes the importance of the variable PR as a means of characterizing the blood flow.

We shall use Taylor's representation with a slight modification: In order that the viscosity will be finite at the lowest value of pressure, a new parameter (S_o) will be used.

$$(7) \quad \mu_{app} = \mu_\infty \left[1 + K(S + S_o)^{-\frac{1}{2}}\right]$$

The value of μ_{app} at zero pressure, $\mu(0)$, will now be:

$$(8) \quad \mu(0) = \mu_\infty \left[1 + K S_o^{-\frac{1}{2}}\right]$$

which is quite large but not infinite.

The representation also agrees with Kumin's data, as shown in Fig. IV. K is close to 0.6 $\left[\frac{(\text{dynes})^{\frac{1}{2}}}{\text{cm}}\right]$, S_o has the value of 2 $\left[\frac{\text{dynes}}{\text{cm}^2}\right]$, and μ_∞ is 0.0333 (poises).

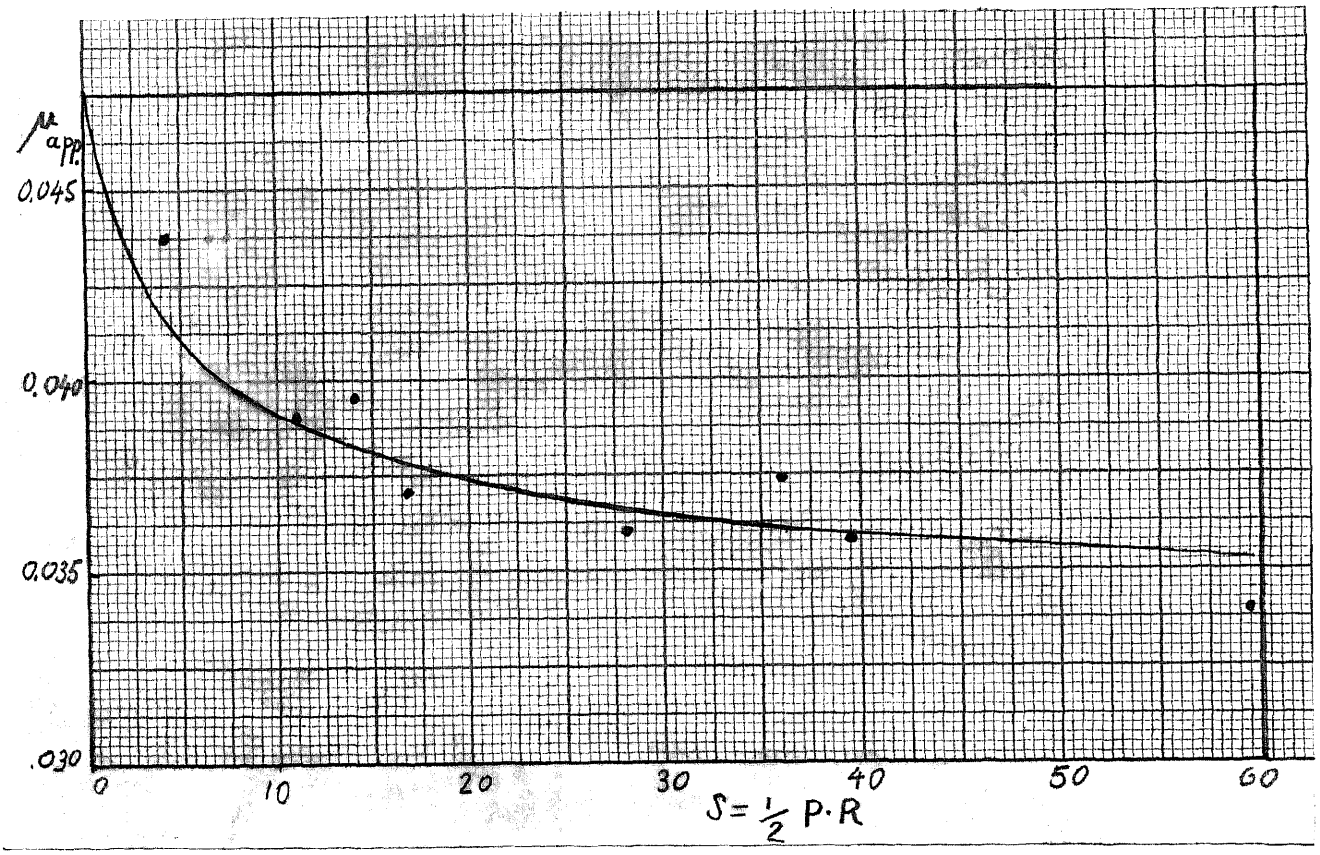

Fig. IV. Data from Table I of Kumin (tube diameter 4.955 mm, hematocrit 40%). The ordinate gives the apparent viscosity in poises, while the abscissa gives the wall stress ($\frac{1}{2}$ PR) in dynes/cm^2. The solid line has the equation $\mu_{app} = 0.0333 \left[1 + 0.6(S + 2)^{-\frac{1}{2}}\right]$. The dots represent the experimental data.

TABLE NO. 1 (For Fig. IV)

Apparent Viscosity Versus Wall Stress

$S = \frac{1}{2}PR$ $(\frac{dynes}{cm^2})$	μ_{app} (Poises)
59.5	0.0339
39.5	0.0358
36.0	0.0374
28.2	0.0351
16.8	0.0371
14.2	0.0395
11.1	0.0391
4.2	0.0438

Data from Kümin's Table I.

Tube diameter 4.955 mm, Hematocrit 40%.

Derivation of the viscosity profile.- If we substitute equation (7) in (5), the expression for the rate of flow becomes:

$$(9)\quad Q = \frac{\pi R^4 P}{8 \mu_{app}} = \frac{\pi R^4 P}{8 \mu_\infty [1+K(S+S_0)^{-\frac{1}{2}}]}$$

The equilibrium condition for steady flow leads to the same differential equation as before (2).

$$\mu \frac{dv}{dr} = -\frac{Pr}{2}$$

However, the viscosity is no longer a constant but depends on the rate of shear or velocity gradient $(\frac{dv}{dr})$.

If we set $s = \frac{1}{2}Pr$ and $g = -dv/dr$, we can write

$$(10)\quad s = \mu(g).g$$

Solving for g

$$(11)\quad g = F(s)$$

The rate of flow through the tube is given by

$$Q = 2\pi \int_0^R r v_{(r)}\, dr$$

integrating by parts gives

$$Q = 2\pi \left[v_{(r)} \frac{r^2}{2}\right]\Big|_0^R - 2\pi \int_0^R \frac{r^2}{2} \frac{dv}{dr}\, dr$$

Setting the boundary condition $v(R) = 0$, the first term will vanish

$$Q = \pi \int_0^R r^2 g\, dr$$

Changing the variable $r = \frac{2s}{P}$, $dr = \frac{2}{P} ds$ yields to

$$Q = \pi \int_0^{\frac{1}{2}PR} \frac{4s^2}{P^2} g \cdot 2 \frac{ds}{P} = \frac{8\pi}{P^3} \int_0^S s^2 F(s)\, ds$$

Q can now be represented by (9)

$$\frac{P^3 Q}{8\pi} = \frac{P^3}{8\pi} \frac{\pi R^4 P}{8 \mu_\infty [1+K(S+S_0)^{-\frac{1}{2}}]} = \frac{S^4}{4 \mu_\infty [1+K(S+S_0)^{-\frac{1}{2}}]} = \int_0^S s^2 F(s)\, ds$$

Differentiating both sides with respect to S

$$\frac{S^3}{\mu_\infty} \left\{ \frac{[1+K(S+S_0)^{-\frac{1}{2}}][\frac{1}{8}S+S_0]}{[1+K(S+S_0)^{-\frac{1}{2}}]^2} \right\} = s^2 F(s)\Big|_0^S = S^2 F(S)$$

Solving for F(S)

$$(12)\quad F(S) = -\left.\frac{dv}{dr}\right|_{r=R} = \frac{S}{\mu_\infty}\cdot\frac{1+K(S+S_0)^{-\frac{3}{2}}\left(\frac{9}{8}S+S_0\right)}{\left[1+K(S+S_0)^{-\frac{1}{2}}\right]^2}$$

And by (11) we find

$$(13)\quad -\frac{dv}{dr} = F(s) = \frac{1}{\mu_\infty}\cdot\frac{1+K(1+S_0)^{-\frac{3}{2}}\left(\frac{9}{8}1+S_0\right)}{\left[1+K(1+S_0)^{-\frac{1}{2}}\right]^2}$$

By integrating $F(S)$ we can find the velocity profile $v(r)$.

The viscosity profile is given by:

$$(14)\quad \mu_{(1)} = \frac{1}{F(1)} = \mu_\infty\cdot\frac{\left[1+K(1+S_0)^{-\frac{1}{2}}\right]^2}{1+K(1+S_0)^{-\frac{3}{2}}\left(\frac{9}{8}1+S_0\right)}$$

Fig. V. shows the distribution of the velocity gradient over the cross-section of the tube which turns to be very close to the linear distribution found for the case of a Newtonian liquid. Hence the velocity profile will again be close to a parabola, and will differ slightly from it in a very narrow region near the center of the tube.

Fig. VI. shows the viscosity profile, which closely resembles the apparent viscosity curve plotted above (broken line) for the equivalent shear values ($P\frac{R}{2}$). The maximum viscosity occurs at the center, and is 1.424 times bigger then the asymptotic value μ_∞.

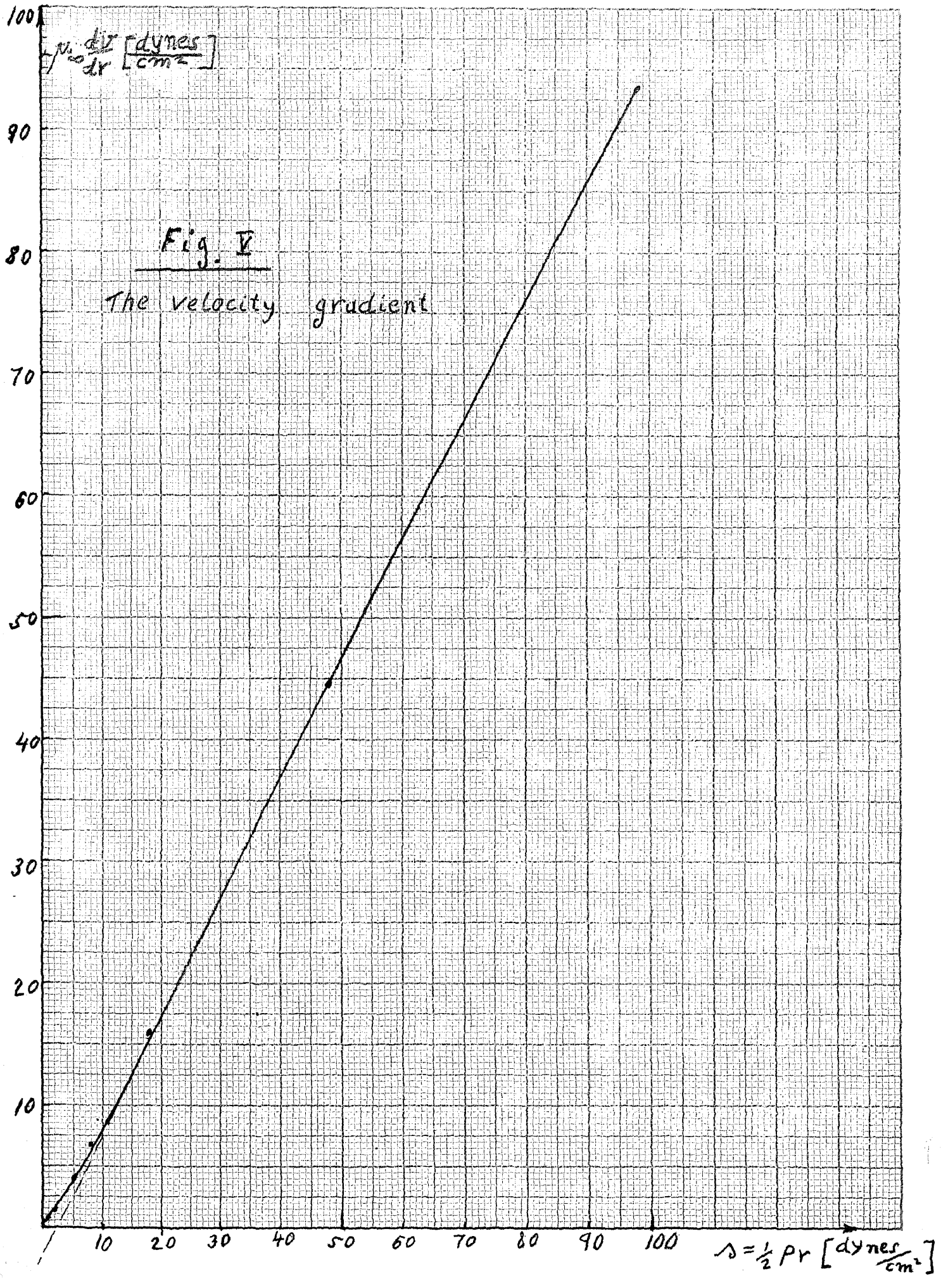

Fig. V

The velocity gradient

Fig. VI

The viscosity distribution

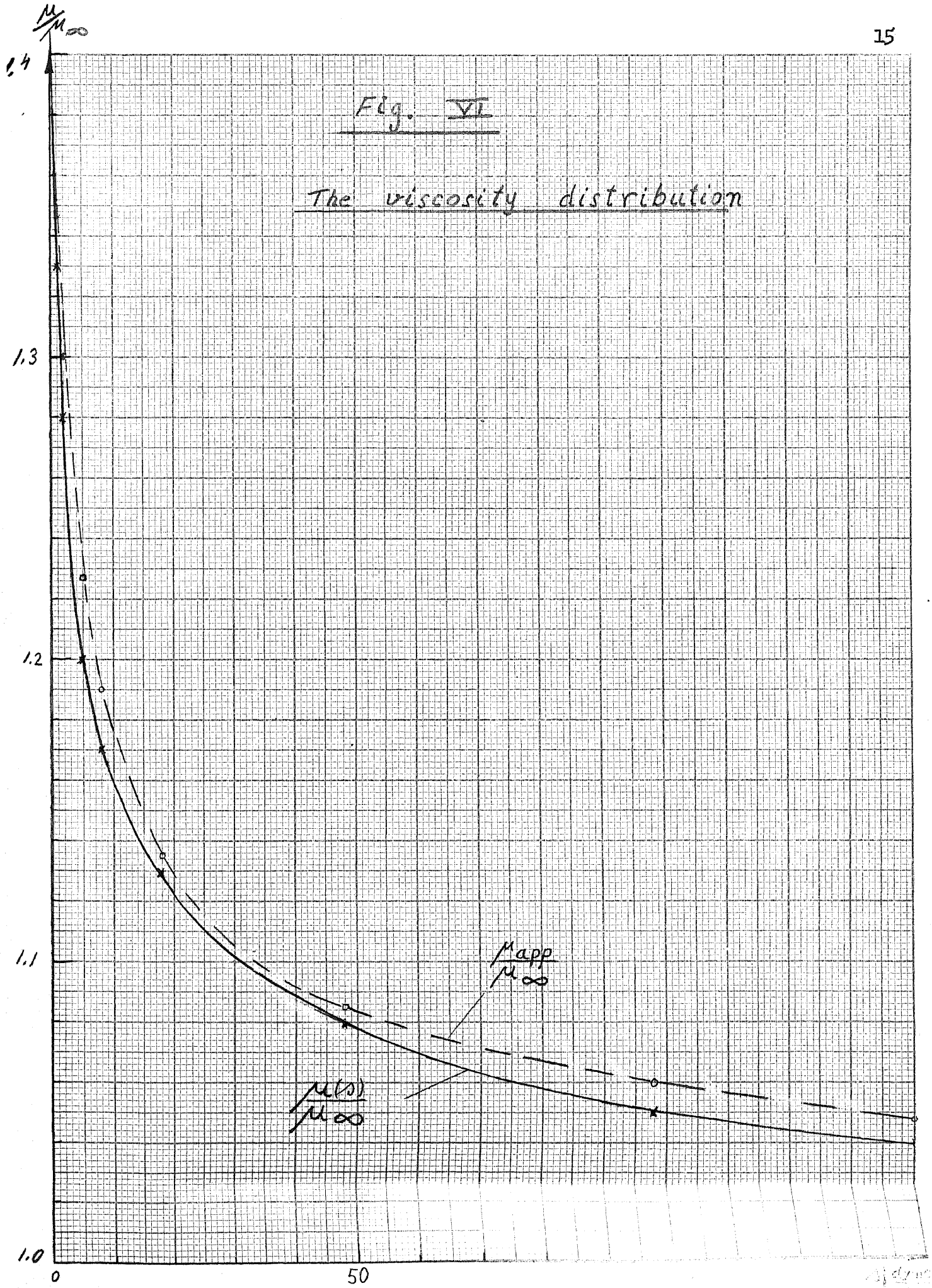

TABLE NO. 2 (For Fig. V, VI)

s $(\frac{\text{dynes}}{\text{cm}^2})$	$\frac{\mu_{app}}{\mu_\infty}$	$-\mu_\infty \frac{dv}{dr}$ $(\frac{\text{Poises}}{\text{sec}})$	$\frac{\mu(s)}{\mu_\infty}$
0	1.424	0.75	1.424
1	1.346	1.565	1.33
2	1.30	4.16	1.28
5	1.227	6.85	1.20
8	1.19	15.9	1.17
18	1.135	44.5	1.13
48	1.085	93.3	1.079
98	1.060		1.05
200	1.0425		1.028
2000	1.020		1.012
	1.000		1.000

Computed by the formulas:

$$(7)\quad \mu_{app} = \mu_\infty \left[1 + K(s+s_0)^{-\frac{1}{2}}\right]$$

$$(13)\quad -\frac{dv}{dr} = \frac{s}{\mu_\infty} \frac{1 + K(1+s_0)^{-\frac{3}{2}}\left(\frac{3}{2}1 + s_0\right)}{\left[1 + K(1+s_0)^{-\frac{1}{2}}\right]^2}$$

$$(14)\quad \mu(s) = \mu_\infty \frac{\left[1 + K(1+s_0)^{-\frac{1}{2}}\right]^2}{1 + K(1+s_0)^{-\frac{3}{2}}\left(\frac{3}{2}1 + s_0\right)}$$

for the values: $K = 0.6\ (\frac{\text{dyne}^{\frac{1}{2}}}{\text{cm}})$; $s_0 = 2(\frac{\text{dynes}}{\text{cm}^2})$

2. The Hematocrit Profile.

In computing the hematocrit profile over the tubes' cross-sectioned area, the following considerations were taken into account.

a) The equilibrium condition between the accumulating force and the scattering "diffusion force".

b) The conservation of the cells' number in a fixed volume.

c) The relation between the viscosity and the hematocrit (near the periphery).

a) The accumulating force which tends to move each particle toward the center of the tube depends upon the rate of shear in the neighborhood of the particle. As previously discussed we can for a first approximation assume linearity between this force and the velocity gradient dv/dr. The random collisions of the cells are too complicated to be accurately described especially in such a dense medium as the blood. For simplicity, we assume the resultant average force due to collisions to be proportional to the density gradient $d\phi/dr$.

In a steady flow, the accumulating force will be equal to the spreading one. This relationship is represented by

$$(15) \quad C \frac{dv}{dr} = \frac{d\phi}{dr}$$

$$\phi(r) = Cv(r) + c'$$

The hematocrit will tend to adopt the profile of the velocity. Remembering that the velocity distribution is close to a parabola, $\phi(r)$ will have the form

$$(16) \quad \phi(r) = A - Br^2$$

The parameters A and B are functions of R and P, and will be computed using the following arguments.

b) At a steady flow the number of cells entering the tube in a second must be equal to the number of cells leaving the tube in the same amount of time. At the output of the tube the total volume of fluid leaving the tube in a unit of time is Q. The volume occupied by cells will therefore be $\phi_o Q$,

$$(17)\quad \phi_o Q = \phi_o \cdot 2\pi \int_0^R v_{(r)}\, r\, dr$$

where ϕ_o is the average hematocrit of the blood. The volume of the cells which pass through any cross-section of the tube is equal to:

$$(18)\quad \int_0^R 2\pi r \cdot \phi(r)\, v(r)\, dr$$

Equating (17) and (18)

$$(19)\quad \phi_o \int_0^R v_{(r)}\, r\, dr = \int_0^R \phi_{(r)}\, v_{(r)}\, r\, dr$$

Substituting $\phi_r = A - Br^2$ and $v = C(R^2 - r^2)$

$$C\,\phi_o\,(R^2 - r^2)r\,dv = C\,(A - Br^2)(R^2 - r^2)r\,dr$$

$$C\,\phi_o\,\frac{R^4}{4} = C\,\frac{R^4}{4}\left(A - \frac{B}{3}R^2\right)$$

We get the following relationship between A and B

$$(20)\quad A = \phi_o + \frac{1}{3}BR^2$$

Substituting in (16) we get

$$(21)\quad \phi = \phi_o + \frac{BR^2}{3}\left(1 - \frac{3r^2}{R^2}\right)$$

At the distance $r = R\,\frac{1}{\sqrt{3}}$ the hematocrit does not change.

c) The effect of concentration on viscosity has been investigated by many workers. Einstein[6] tried to estimate molecular dimensions by gas viscosity. He obtained the following formula:

$$(22)\quad \frac{\mu}{\mu_o} = 1 + 2.5\,\phi$$

where μ is the viscosity of the suspension,

μ_o = the viscosity of the pure medium containing the particles,

ϕ = the volume ratio of the particles to the total fluid.

The above formula, derived for a very dilute system, also agrees with Jeffery's method of finding the viscosity by computing the amount of energy dissipation associated with each particle.

J. Happel[7], using hydrodynamic considerations, evolved the formula:

$$(23)\quad \frac{\mu}{\mu_o} = 1 + 5.5\,\phi\,\frac{4\phi^{7/3} + 10 - 84/11\,\phi^{2/3}}{10(1 - \phi^{10/3}) - 25\phi(1 - \phi^{4/3})}$$

This formula is in a good agreement with data on suspensions of small spherical particles up to concentrations of 40 to 50 per cent by volume of solids. Above this concentration, particles are no longer free to move with respect to each other, and friction due to inter-particle contacts will result in a higher viscosity than that which was predicted from purely hydrodynamic considerations.

In Fig. VII equation (23) is plotted together with an experimental blood viscosity curve deduced from Haynes[2] data. Fig. VII shows that as the concentration approaches a certain limit, the viscosity goes up to infinity. From geometrical reasons this limit will be $\phi = 0.53$ for spheres, and 0.785 for circular discs.

The average hematocrit of normal human blood is $\phi = 0.4$. From the graph of Fig. VII it can be seen that below this value the viscosity-density curve is quite linear, while above $\phi = 0.4$ it resembles an exponential curve. A small increase in hematocrit will result in a

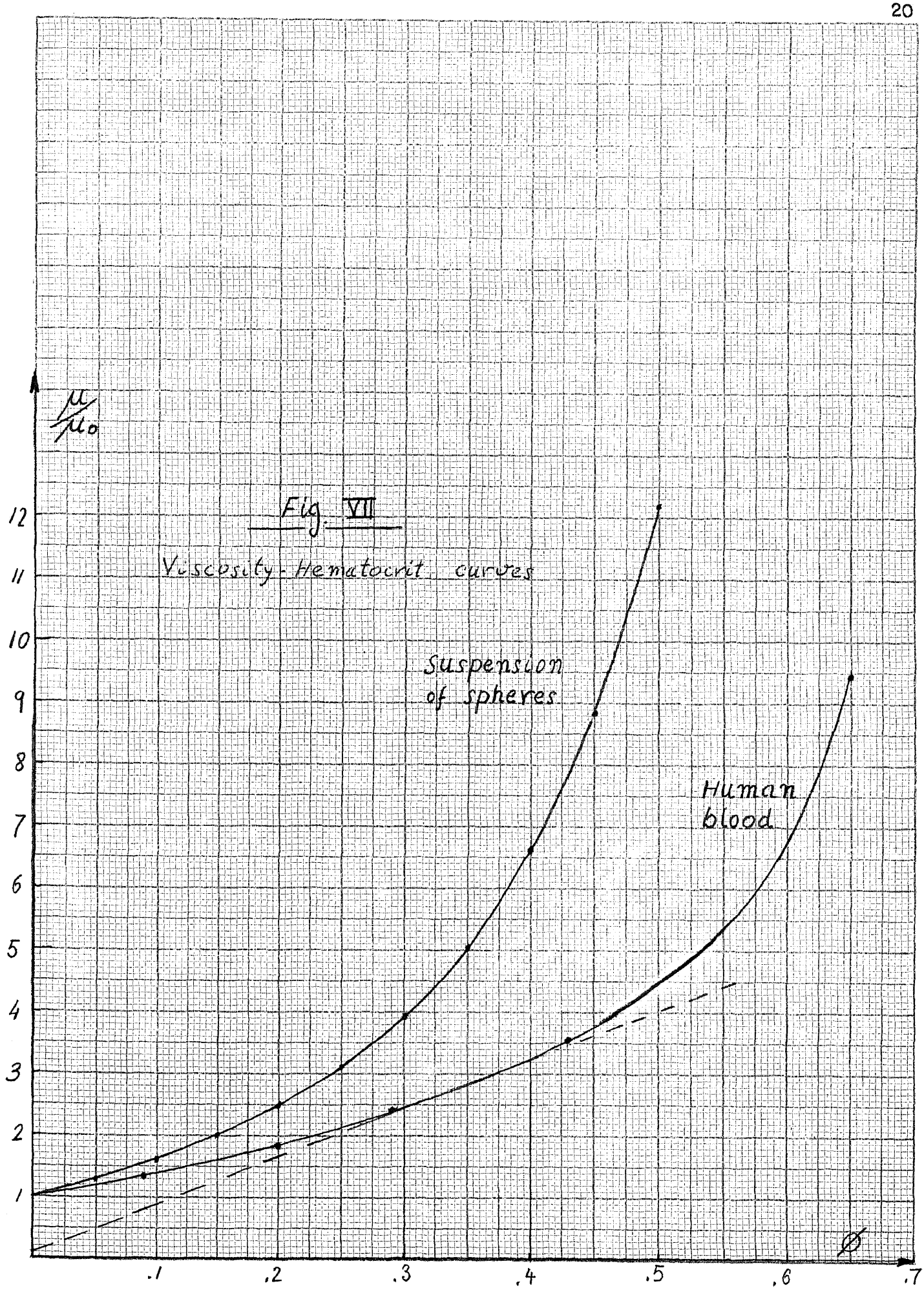

Fig. VII

Viscosity - Hematocrit curves

TABLE NO. 3 (For Fig. VII)

Viscosity Versus Hematocrit

Suspension of spheres		Human blood	
ϕ %	$\frac{\mu}{\mu_o}$	ϕ %	$\frac{\mu}{\mu_o}$
0	1.000	0	1.00
5	1.281	9	1.31
10	1.605	20	1.81
15	1.997	29	2.43
20	2.486	43	3.55
25	3.115	65	9.45
30	3.942		
35	5.062		
40	6.621		
45	8.861		
50	12.200		

The data for suspension of spheres was obtained by Happel's formula

$$(23)\ \frac{\mu}{\mu_o} = 1 + 5.5\phi\ \frac{4\phi^{\frac{7}{3}} + 10 - \frac{84}{11}\phi^{\frac{2}{3}}}{10(1-\phi^{\frac{10}{3}}) - 25\phi(1-\phi^{\frac{4}{3}})}$$

The data for human blood was derived from Haynes[2] data (Fig. I).

large increase in viscosity. In order to make use of the linear relationship between viscosity and hematocrit, we shall apply it only at the periphery of the tube, where the hematocrit drops below the average, and therefore it is in the linear range. The linear representation is also justified by the fact that the maximum viscosity change is 30% (Fig. VI). This is caused by hematocrit variations of a maximum of 12%. The latter are still in the linear range. The linear approximation of the viscosity-hematocrit curve, in the range between $\phi = 0{,}4$ and $\phi = 0{,}3$, is expressed in the formula,

$$(24)\quad \frac{\mu}{\mu_o} = 8.00\,\phi + 0.107$$

Near the point $\phi = \phi_0 = 0{,}4$ the straight line can be approximated again by neglecting the constant term 0.107.

$$(25)\quad \frac{\mu}{\mu_o} = 8.00\,\phi \qquad \text{or} \qquad \phi = C\,\mu$$

The error involved is no greater than 3%. Instead of using the parameter μ_o, the viscosity of pure plasma, we shall use $\mu(0)$, the viscosity when the blood is at rest. Assuming that at rest the cells are uniformly distributed and therefore $\phi = \phi_0$, we have the condition

$$\phi_0 = C \cdot \mu(0)$$

$$\text{therefore } C = \frac{\phi_0}{\mu(0)}$$

Substituting in (25)

$$\phi = \frac{\phi_0}{\mu(0)} \qquad \text{or}$$

$$(26)\quad \phi\,(R,P) = \frac{\phi_0}{\mu(0)}\,\mu(R,P)$$

where $\mu(R,P)$ is the viscosity at the periphery, and can be found by substituting r = R into the viscosity distribution function (14).

$$(14a) \qquad (R,P) = \frac{\mu_\infty \left[1 + K\left(\frac{PR}{2} + S_o\right)^{-\frac{1}{2}} - \right]^2}{1 + K\left(\frac{PR}{2} + S_o\right)^{-\frac{3}{2}}\left(\frac{9}{8}\frac{PR}{2} + S_o\right)}$$

In order to find the parameter $B(R,P)$ we substitute $r = R$ in (21) and equate with (26).

$$\underset{(r=R)}{\phi} = \phi_o - \frac{2}{3} BR^2 = \frac{\phi_o}{\mu(0)} \mu(R,P)$$

$$B\frac{R^2}{3} = \frac{\phi_o}{2}\left(1 - \frac{\mu(R,P)}{\mu(0)}\right)$$

Substituting $\frac{BR^2}{3}$ in (21) gives the final density distribution function

$$(27) \quad \phi = \phi_o + \frac{\phi}{2}\left(1 - \frac{\mu(R,P)}{\mu(0)}\right)\left(1 - \frac{3r^2}{R^2}\right)$$

Fig. VIII shows the distribution for several values of the applied wall stress, $S = \frac{PR}{2}$.

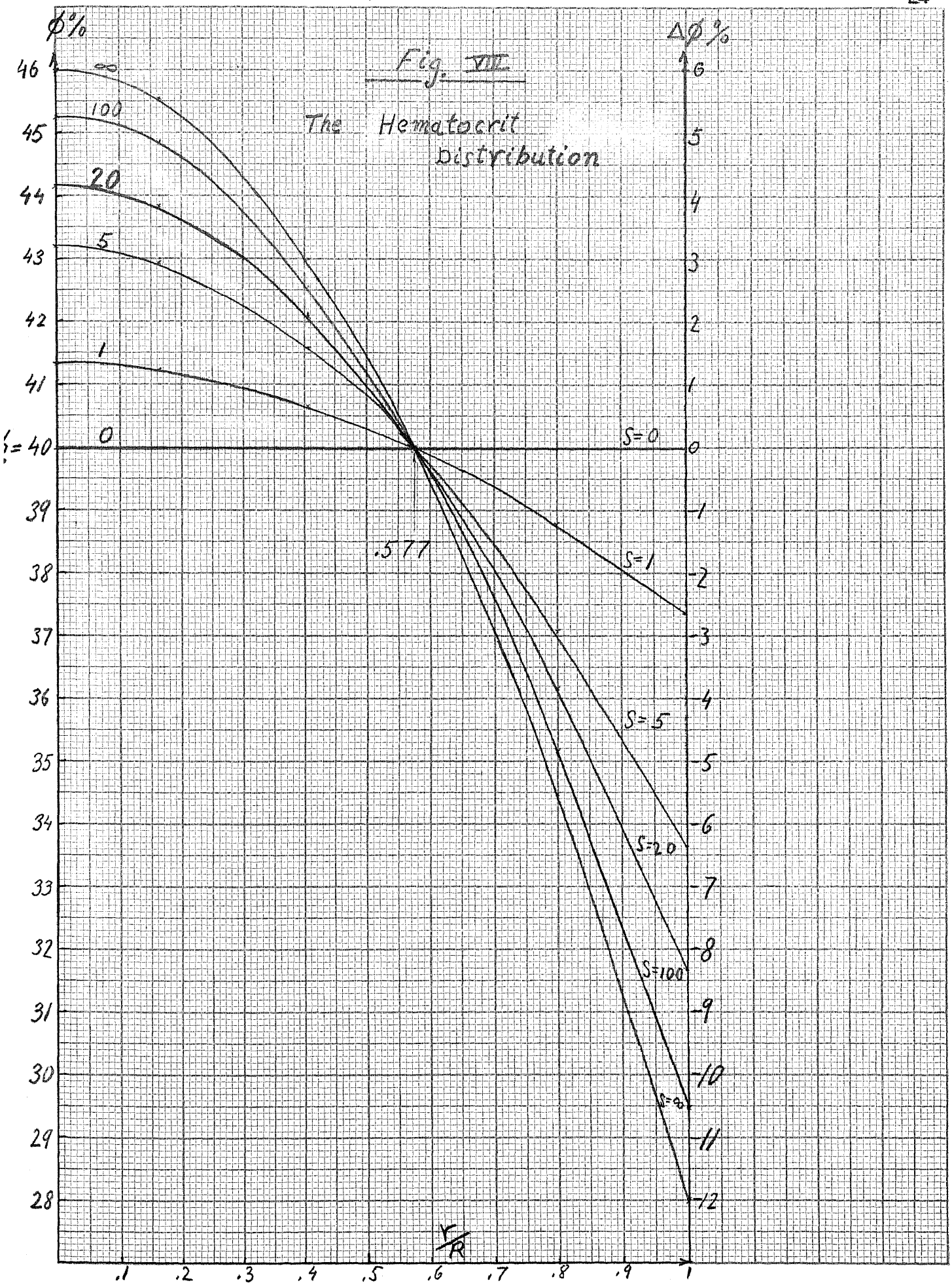
Φ%
ΔΦ%
Fig. VII
The Hematocrit distribution
∞
100
20
5
1
0
S=0
S=1
S=5
S=20
S=100
S=∞
.577
r/R
46
45
44
43
42
41
40
39
38
37
36
35
34
33
32
31
30
29
28
6
5
4
3
2
1
0
-1
-2
-3
-4
-5
-6
-7
-8
-9
-10
-11
-12
.1
.2
.3
.4
.5
.6
.7
.8
.9
1

3. The Effect of Cell Distribution on the Electrical Conductance.

Before studying the change of blood conductance for the particular cell distribution of flowing blood, the behavior of the conductance for different types of distribution will be discussed on a qualitative basis.

a) Blood at rest. It will be proved that the conductivity of blood has a stationary value for a uniform distribution of cells. When the medium is a better conductor then the cells, of all the possible configurations, a uniform distribution will result in the highest resistivity, which means that any disturbance in the uniform density of the cells will result in an impedance drop.

Let us consider a tube 1 meter long, with a cross sectional radius R. The specific conductivity (g) is a function of the distance (r) from the center.

$$g(r) \text{ in } \frac{\text{mhos}}{\text{meter}}$$

The total longitudinal conductance of the tube will be

$$(28)\quad G = 2\pi \int_0^R g(r)\, r\, dr$$

The specific conductivity g is a function of the density of the cells, ϕ

$$(29)\quad g = f(\phi)$$

The density ϕ is again a function of r, and if the total number of cells in the tube does not change, the average hematocrit ϕ_0 is constant.

$$(30)\quad \phi_0 = \frac{2\pi}{\pi R^2} \int_0^R r\, \phi(r)\, dr$$

The problem before us is to find what density function $\phi(r)$ will minimize the conductance.

$$G = 2\pi \int_0^R f(\phi) r \, dr$$

subject to the constraint

$$I_1 = \int_0^R r \, \phi(r) \, dr = \frac{R^2}{2} \phi_0 = \text{constant}$$

To solve this problem, we consider the integral

$$(31) \quad I_0 = \int_0^R F_0(r, \phi) dr$$

where

$$(32) \quad F_0 = r \cdot f(\phi) + r\phi(r)$$

λ is a parameter to be determined.

Since the integral I_1 must remain constant, the integral I_0 will be stationary only if G is stationary. The Euler differential equation that satisfies the above conditions is:[8]

$$(33) \quad \frac{\partial F_0}{\partial \phi} - \frac{d}{dr}\left(\frac{\partial F_0}{\partial \phi'_r}\right) = 0$$

F_0 does not include the derivative of ϕ with respect to r, and therefore

$$\frac{\partial F_0}{\partial \phi'_r} = 0$$

and equation (33) becomes

$$(34) \quad \frac{\partial F_0}{\partial \phi} = rf'(\phi) - \lambda r = 0$$

$$(35) \quad f'(\phi) = \lambda$$

Therefore ϕ = constant = ϕ_0 for any function $f(\phi)$.

b) Flowing blood. When the fluid is moving through the tube the condition which is imposed on the cells is not that the total number of cells in a certain area of the tube remains unchanged but that

the number of cells passing through any cross section of the tube per unit time is constant or,

$$(36)\quad Q\,\phi_o = 2\pi \int_o^R r\,\phi(r)\,v(r)\,dr$$

$\phi(r)$ is now subject to another constraint.

$$(37)\quad I_2 = \int_o^R r\,\phi(r)\,v(r)\,dr = \text{constant}$$

F_o becomes

$$(38)\quad F_o = r\,f(\phi) + \lambda\, r\,\phi(r)\,v(r)$$

and Euler equation becomes

$$(39)\quad \frac{\partial F_o}{\partial \phi} = r\,f'(\phi) + \lambda\, r\,v(r) = 0$$

$$(40)\quad f'(\phi) = -\lambda\,v(r)$$

$f'(\phi)$ is always negative since an increase in the number of cells must result in less conductivity of the fluid. However, $v(r)$ reaches zero at $r = R$, and in order for $f'(\phi)$ to reach zero, ϕ must approach infinity at this point. Consequently the function $(\phi)r$ which will minimize the conductance is a function having a singularity at the periphery, or $\phi(R) \to \infty$.

But ϕ can never exceed the value of 1. Therefore, the derived distribution function cannot exist. This result is explained by the fact that the net conductance is minimized when the total number of cells in the cross sectional area is maximal. This condition will be attained when the majority of the cells are concentrated at the periphery where the velocity is least.

The reason is that the number of cells entering and leaving the tube must be equal, and in the above state the majority of cells involved in the exchange are moving at low velocities. As a result the

required number of cells in the cross-section must be greater in order to compensate for the lower velocities. In contrast, when the majority of the cells accumulates in the axial stream where the velocity is high, the required exchange of cells is accomplished with lower total cross sectional concentrations. In other words, the average hematocrit in the tube is lower than the average hematocrit in the blood reservoir, and the conductance is greater.

The reduction of the average hematocrit of flowing blood can be quantitatively shown for the case where the velocity and the hematocrit both have a parabolic profile. If according to (3)

$$v = C_1 \left(1 - \frac{r^2}{R^2}\right)$$

then according to (21) condition (19) is satisfied by

$$\phi = \phi_o + C_2 \left(1 - \frac{3r^2}{R^2}\right)$$

and the average hematocrit in the tube is

$$\phi_{av} = \frac{2}{R^2}\int_o^R r\,\phi(r)\,dr = \frac{2}{R^2}\int_o^R \left[\phi_o + C\left(1 - \frac{3r^2}{R^2}\right)\right] .r\,dr = \phi_o - \frac{C_2}{2}$$

The change in the average hematocrit is therefore negative

$$\phi_{av} - \phi_o = -\frac{C_2}{2}$$

and using (27) the amount of reduction is

$$\frac{C_2}{2} = \frac{\phi_o}{4}\left[1 - \frac{\mu(R,P)}{\mu(0)}\right]$$

Maxwell's formula and its limitations. In the preceeding discussion the relationship between the conductivity and the hematocrit, $f(\phi)$, remained undetermined. The problem of calculating the conductivity of a heterogenous system was first solved by J. C. Maxwell[9] using the following argument.

Consider a sphere having a specific conductivity g_2 being surrounded by a medium with a specific conductivity g_1. If a uniform electric field (E_o) is applied to this model, the field distribution will not be uniform because of the non-uniformity of the conductivity. The boundary conditions which the actual field must satisfy are:

1) The electric field must be uniform at infinity

2) The potential must be continuous at the surface of the sphere

$V_1(a) = V_2(a)$

3) The normal component of the current density (j) must be continuous at the surface of the sphere.

$$g_1 \frac{\partial V_1}{\partial r} = g_2 \frac{\partial V_2}{\partial r} \qquad (r = a)$$

Where V_1 and V_2 are the potentials inside and outside the sphere respectively, and a is the radius of the sphere. These boundary conditions are fulfilled if the field outside the sphere is considered as being produced by the applied field (E_o), and by a dipole placed in the center of the sphere having the intensity

$$(41)\quad M = E_o \frac{g_1 - g_2}{2g_1 + g_2} a^3$$

and when the field inside the sphere is uniform and equal to

$$(42)\quad E_2 = E_o \frac{3g_1}{2g_1+g_2}$$

The resultant potential at any point outside the sphere and in a distance r from its center is given by

$$(43)\quad V_1 = E_o \cos\theta \left(r + \frac{g_1 - g_2}{2g_1+g_2} \cdot \frac{a^3}{r^2}\right)$$

where θ is the angle between the applied field and the radius vector r.

If n spheres are placed in a unit volume of the medium, the potential at a great distance from a certain element of volume can be considered as being produced by n dipoles all placed at its center, and will therefore be equal to:

$$(44)\quad V_1 = E_o \cos\theta \left(r + \frac{g_1 - g_2}{2g_1+g_2} \cdot \frac{a^3}{r^2}.n\right)$$

But a^3 is the volume ratio of the spheres to the total volume $a^3n = \phi$

Equation (44) can be written as

$$(45)\quad V_1 = E_o \cos\theta \left(r + \frac{g_1 - g_2}{2g_1+g_2} \cdot \frac{\phi}{r^2}\right)$$

An equivalent homogenous sphere which can replace the volume element and will result in the same field must have a specific conductivity g which satisfies the equation:

$$(46)\quad \frac{g_1 - g}{2g_1 + g} = \frac{g_1 - g_2}{2g_1 + g_2}\phi$$

The equivalent conductivity g of the system is therefore

$$(47)\quad g = g_1 \frac{2g_1 + g_2 - 2\phi(g_1 - g_2)}{2g_1 + g_2 + \phi(g_1 - g_2)}$$

In human blood the conductance of the red cells (g_2) is negligable with respect to the conductivity of the plasma (g_1), and equation (47) becomes

$$(48)\quad g = 2g_1 \frac{1 - \phi}{2 + \phi}$$

It is important to mention the basic assumptions this argument was based upon.

1) The system was constituted of homogenous perfect spheres, and therefore the volume ratio (ϕ) was the only parameter, excluding the effect of orientation which takes place when the solids are not perfect spheres.

2) The distances between the spheres were considered big enough so that the field near one of them was not effected by its neighbors. The boundary conditions which were imposed on the electric field were sufficient only under this assumption. The continuity of the electric current at the surface of separation is fulfilled by superposition of the applied uniform field and a dipole at the center of that sphere, but will no longer hold when dipoles are placed in the environment. If the effect of close spheres has to be taken into account, a forth boundary condition should be fulfilled; the current normal to the plane of symmetry between any two spheres must vanish.

The conductance calculation. Applying Maxwell's formula (48) for conductivity of a dispersed system of non-conductive spheres,

$$g = 2g_1 \frac{1 - \phi}{2 + \phi} = 2g_1\left(\frac{3}{2 + \phi} - 1\right)$$

where (g) is the equivalent specific conductivity of the system, and (g_1) is the specific conductivity of the conducting medium (plasma). The average conductance of the tube is:

$$(49)\quad G_o = \frac{2}{R^2}\int_0^R r\, g(r)\, dr$$

The density distribution function $\phi(r)$ is given by (27)

$$(50)\quad \phi(r) = C_1 - C_2 r^2$$

where $C_1 = \frac{\phi_o}{2}\left(3 - \frac{\mu(s)}{\mu(o)}\right)$ and $C_2 = \frac{3\,\phi_o}{2R^2}\left(1 - \frac{\mu(s)}{\mu(o)}\right)$

Substituting (50) in (49)

$$(51)\quad G_o = \frac{2}{R^2}\int_0^R r\, 2g_1\left(\frac{3}{2 + C_1 - C_2 r^2} - 1\right)dr = \frac{12g_1}{R^2} I - 2g_1$$

where $I = \int_0^R \frac{r\, dr}{2+C_1 - C_2 r^2} = \frac{1}{2C_2} \log \frac{2 + C_1}{2+C_1 - C_2 R^2} =$

$$= \frac{R^2}{3\,\phi_o\left(1 - \frac{\mu(s)}{\mu(o)}\right)} \log_e \frac{2 + \frac{\phi_o}{2}\left(3 - \frac{\mu(s)}{\mu(o)}\right)}{2 + \frac{\phi_o}{2}\left(3 - \frac{\mu(s)}{\mu(o)}\right) - \frac{3}{2}\phi_o\left(1 - \frac{\mu(s)}{\mu(o)}\right)}$$

Substituting in (51):

$$(52)\quad G_o = 2g_1 \frac{2}{\phi_o\left(1 - \frac{\mu(s)}{\mu(o)}\right)} \log_e \frac{2 + \frac{\phi_o}{2}\left(3 - \frac{\mu(s)}{\mu(o)}\right)}{2 + \frac{\phi_o}{2}\left(3 - \frac{\mu(s)}{\mu(o)}\right) - \frac{3}{2}\phi_o\left(1 - \frac{\mu(s)}{\mu(o)}\right)} - 1$$

From the last formula the average conductance (G_o) can be plotted as a function of the applied wall stress $S = \frac{PR}{2}$. The value $\frac{\mu(s)}{\mu(o)}$ can be found according to Fig. VI. When the blood is at rest $\frac{\mu(s)}{\mu(o)} = 1$ and at this point,

$$\lim_{\mu(s) \to \mu(o)} G_o = 2g_1\left(\frac{3}{2 + \phi_o} - 1\right) = 2g_1 \cdot 0.25$$

as is expected.

In Fig. IX the relative change of G_o will be plotted instead of G_o

$$(53)\quad \frac{\Delta G_o}{G_o} = \frac{G_o(S) - G_o(0)}{G_o(0)}$$

Fig. IX indicates a maximum change of 6.58% in the average conductance, at infinite rate of flow. The graph also indicates a clear saturation which occurs above $S = 20\left[\frac{\text{dynes}}{\text{cm}^2}\right]$.

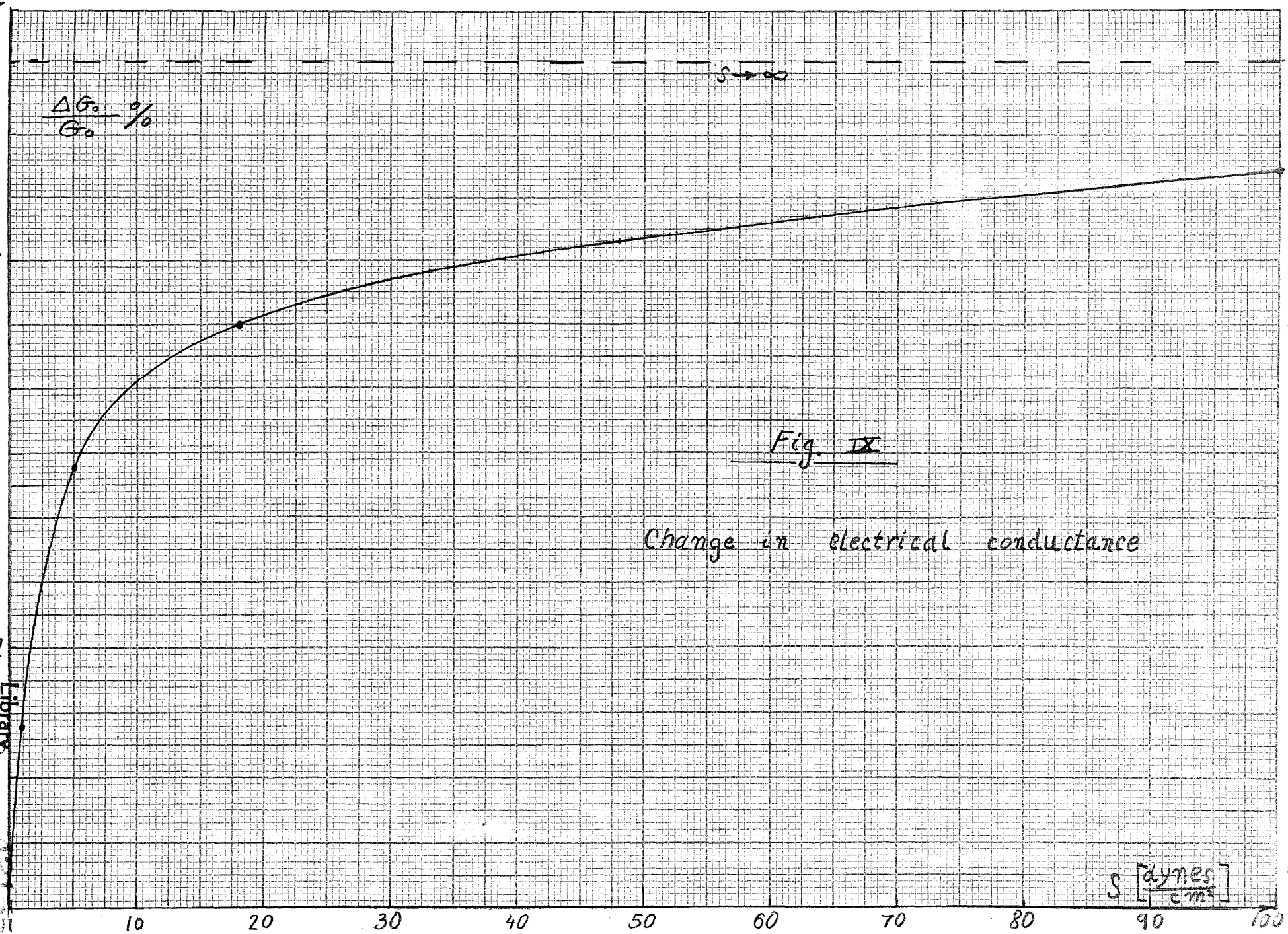

Fig. IX

TABLE NO. 4 (For Fig. IX)

Relative Change in Conductance Versus Applied Wall Stress

$S \frac{dynes}{cm^2}$	$\frac{\Delta G_o}{G_o}$ %
0	0
1	1.395
5	3.40
18	4.49
100	5.72
	6.58

Obtained by formula (52) and (53)

$$(52)\quad G_o = 2g_1 \frac{2}{\phi_o \left(1 - \frac{\mu}{\mu_{(o)}}\right)} \log_e \frac{2 + \frac{\phi_o}{2}\left(3 - \frac{\mu}{\mu_{(o)}}\right)}{2 + \frac{\phi_o}{2}\left(3 - \frac{\mu}{\mu_{(o)}}\right) - 3/2\ \phi_o\left(1 - \frac{\mu}{\mu_{(o)}}\right)} - 1$$

$$(53)\quad \frac{\Delta G_o}{G_o} = \frac{G(s) - G(0)}{G(0)}$$

for $\phi_o = 40\ \%$

CHAPTER II

THE EFFECT OF CELL'S ORIENTATION ON THE CONDUCTIVITY OF BLOOD.

The Hydrodynamic Problem.

In the preceeding chapter (Fig. III) it was shown that a spherical solid placed in a viscous fluid is subjected to translatoric pressure acting parallel to the viscosity gradient, and to a couple acting in the direction of the vorticity lines.* The direction of the velocity gradient for a fluid moving in a tube is radial while the vorticity lines are azimuthal and therefore spherical solids will tend to accumulate toward the center of the tube and rotate around an azimuthal axis.

Dealing with non-spherical solids such as ellipsoidal spheroids the question arises whether these are the only forces acting on the solids, or whether other forces exist which tend to arrange the solids in a particular orientation with respect to the vorticity lines.

This problem was first presented by G. B. Jeffery (1922) who by stating the hypothesis of minimum dissipation of energy came to the conclusion that a second couple is operating on the solids forcing them to line up in a position which causes the minimum energy dissipation. In the case of ellipsoidal spheroids this position is obtained when the axis of symmetry is parallel to the vorticity lines.

*The vorticity lines are the lines perpendicular to the velocity and to the velocity gradient at any point. They are parallel therefore to the vector $\vec{V} \times \overrightarrow{\text{grad}}\ V$.

Many workers tried to observe this phenomena by constructing different types of models but the results were inconclusive. Saffman[10] examined ellipsoidal spheroids between two rotating concentric cylinders and observed a preferred orientation after more than six minutes of rotation. Again examining Jeffery's equations, he came to the conclusion that the effect described by Jeffery is too small to account for this phenomena, and referred it to the inertia terms which Jeffery neglected. As a conclusion the orientation of the ellipsoid is mainly dependent on its initial position and a preferred orientation is attained only after a long time.

At this point it is important to mention another factor which was not considered by Saffman and which concerns a multi-particle system such as human blood. In such a system particles are never in complete equilibrium because of repeated random collisions between them which results in a continuous change of momentum. But some of the particles are more stable than the others in the sense that more force is required to change their position. All the particles are forced to rotate around the vorticity lines, but those which are able to do so around the axis of higher moment of intertia are less effected by random collisions, and will continue their rotation about this axis undistrubed. The moment of inertia of a circular disc with respect to its axis of symmetry is two times greater than the moment of inertia with respect to an axis coinciding with one of its diameters. As a result more cells will be found with their axis of symmetry lying in the direction of the vorticity lines than in any other direction.

Experimental evidence. An experiment was set which as far as blood is concerned proves three points:

1) Red blood cells do prefer a certain orientation when the blood is moving.
2) The preferred orientation is such that the axis of symmetry coincides with the vorticity lines.
3) The preferred orientation is attained the moment the blood starts to move.

Citrated human blood was driven by a dual-cyclic pump through a flat walled chamber 1 mm. in height. The chamber was constructed of transparent plastic and the volume was fixed. A narrow light source threw light on one of the chamber's walls, while a photo-transistor was attached to each side of the chamber in order to detect the intensity of the reflected and transmitted light. The electric signals from the photo-transistors were recorded simultaneously with a signal from a flowmeter indicating the velocity pulse.

The results are shown in Fig X. The light transmitted through the blood has the same shape as the velocity pulse which means that more light is transmitted when the blood is moving than when the blood is at rest. However, the light reflected from the blood has exactly the opposite shape to the transmitted one which means that more light is reflected when the blood is at rest than when the blood is moving.

Fig. XI presents a magnified model which will help to explain the observed phenomena. The upper portion of Fig. XI represents the blood at rest. The red blood cells are in random orientation, and a certain

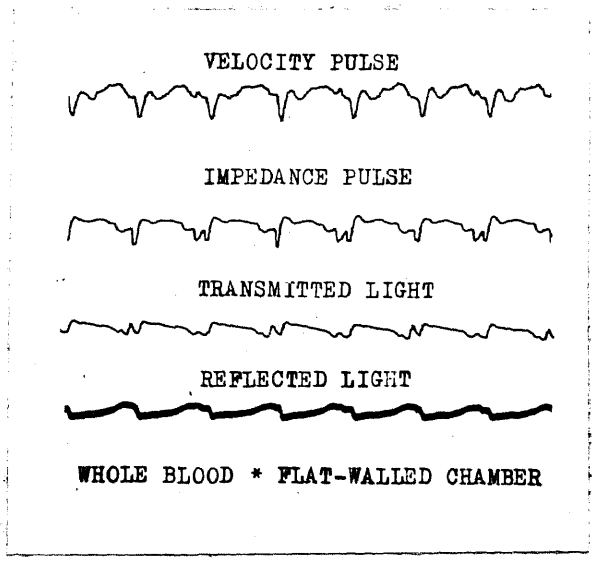

Fig. X

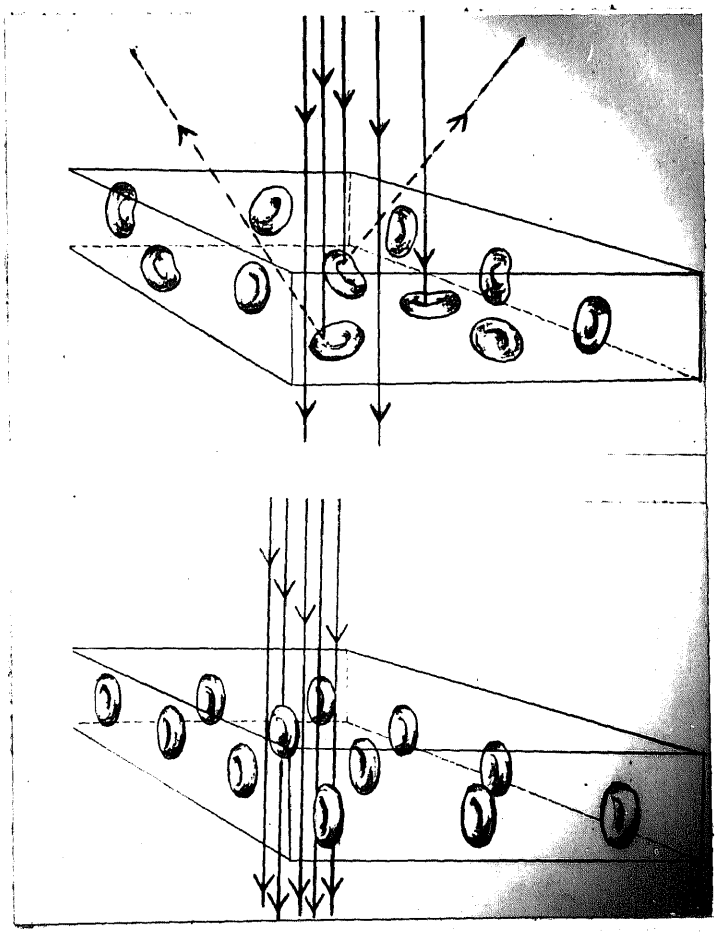

Fig. XI Orientation of Blood Cells in Flat Walled Chamber

amount of light energy is absorbed in the cells which have a higher optical density than the plasma, another part of the energy is reflected back from the cells, and a third part is transmitted through the plasma to the other side of the chamber. The lower picture represents moving blood; the red cells are arranged with their narrow side against the light source, a smaller number of light beams has to pass through the cells and therefore the transmitted light is increased and the reflected and absorbed light is decreased.

In order to be sure that the light variations are only due to orientation of the cells and are not caused by any mechanical vibrations or wiping effect, the same experiment was done with hemolyzed blood where the red cells lose their rigid structure and their content is mixed with the plasma. The transmitted light did not change as shown in Fig. XII. (The spikes which occurred on the transmitted light tracing are due to sediment passing in front of the phototransistor.)

The blood velocity in the flat-walled chamber is zero at the walls and maximal in the middle of the chamber. The vorticity lines are therefore horizontal lines perpendicular to the direction of flow. When the blood is moving the cells are so oriented that their axis of symmetry is parallel to the vorticity lines as is shown in Fig. XI. In analogy, the blood cells in a circular tube will set their axis of symmetry in an azimuthal direction. (Fig. XIII)

Fig. X shows a complete synchronization between the light pulse and the velocity pulse (1 cyc/sec) which indicates that the orientation

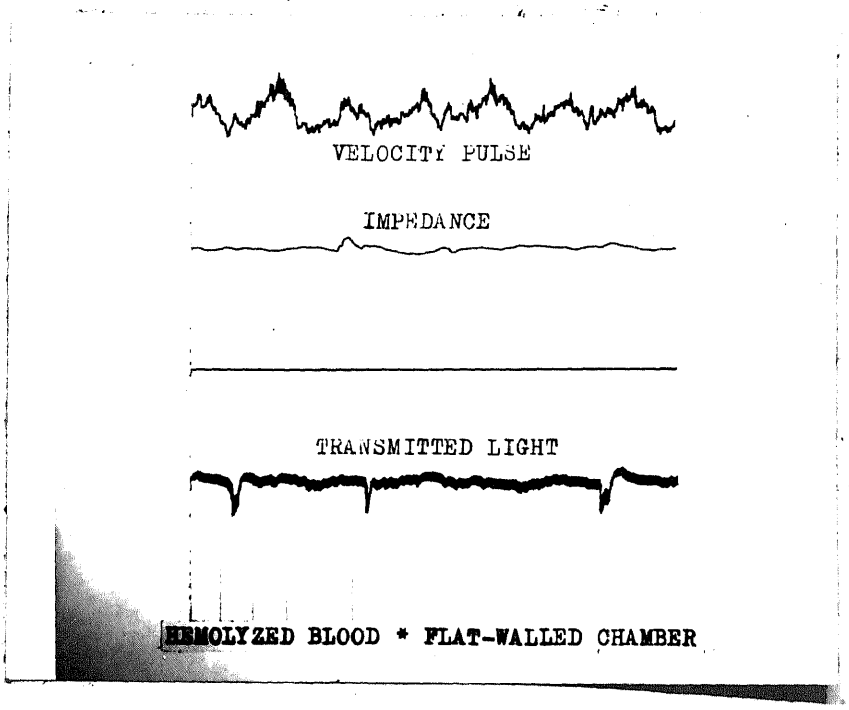
VELOCITY PULSE
IMPEDANCE
TRANSMITTED LIGHT
HEMOLYZED BLOOD * FLAT-WALLED CHAMBER

Fig. XII

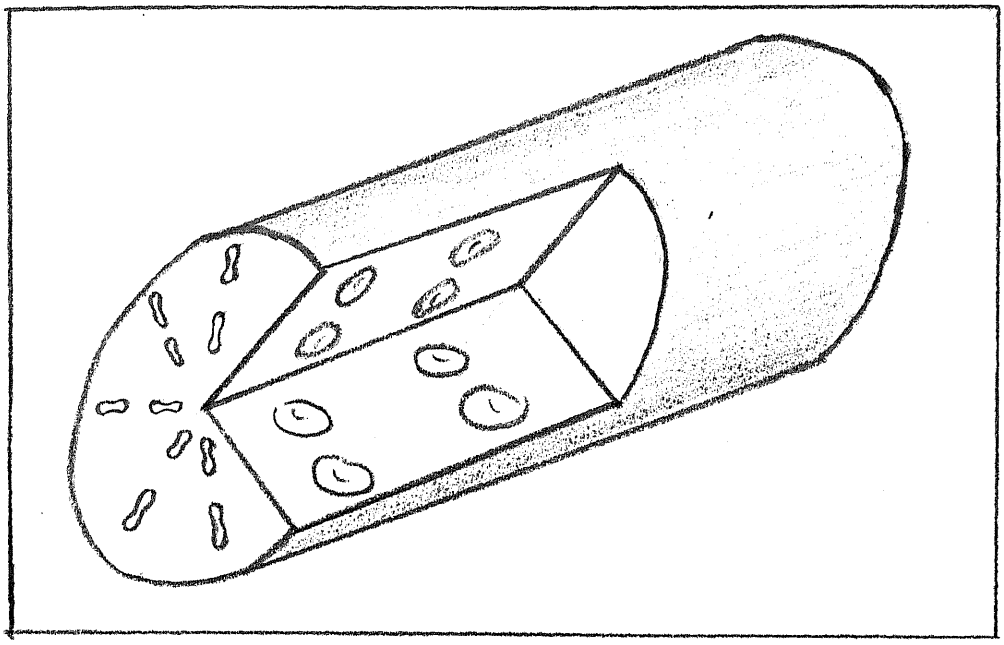

Fig. XIII orientation of blood cells in a circular tube

process occurs together with the blood flow. Consequently this phenomena is essentially different from that observed by Saffman which required a time constant of more than six minutes.

The Resultant Conductivity.

The change of conductivity as a result of change in the angle between the cells and the applied electrical field is quite apparent. When the cells line up with their narrow edges facing the electrical field the total current flowing between the cells is greater than that flowing when their surfaces are facing the field.

The exact function of conductivity versus angular positions of the cells can be worked out by several methods. The direct method which was carried out by Hugo Fricke[11] involves exact solution of Laplace's equation for a model of a single ellipsoidal spheroid between two parallel infinite plates. Having the electric field at any point in space, the ratio between the total current and applied voltage can be calculated. Unfortunately, Laplace's equation can be solved only for those particular cases where the applied electrical field is parallel to one of the three principal axes of the ellipsoid. Furthermore, assuming the above boundary conditions, namely that the distance between the cells is much larger than their diameter, is far from representing blood where the diameter of the cell may occupy up to 80% of the total distance between two neighboring cells.

Better results might be obtained by an indirect method, first put forth by Lord Raleigh[12]. Since the current density distribution that

satisfies Laplace's equation is the one which results in minimum heat dissipation (or maximum total resistance for a given voltage) the resistance is stationary for this distribution of current density. Near a stationary position the change of resistance due to a deviation of the density current function will be very small. This fact permits us to calculate the resistance by assuming any arbitrary current density function which satisfies the boundary conditions.

The resistance computed through this function is fairlyy close to the actual one, even if the function is only close to satisfying Laplace's equation. However, the current density function which fulfills those boundary conditions is quite complicated and the calculation of resistance can hardly be accomplished in terms of elementary functions.

In order to approach actual boundary conditions, the following experimental method was carried out.

A non-conductive circular disc was placed in a cubic-shaped bath (Figure XIV) of conductive liquid. A uniform applied electrical field was produced by aluminum plates covering two opposite walls of the cubic container, while the other walls were insulators. The boundary conditions imposed by the non-conductive walls are identical to those produced by many particles uniformly distributed around the observed cell. The ratio between the disc diameter and the side of the cube was .725 and the ratio of the width of the disc to its diameter was 0.24. The electrical impedance between the plates was measured as a function of the angle between the applied electrical field and the axis of

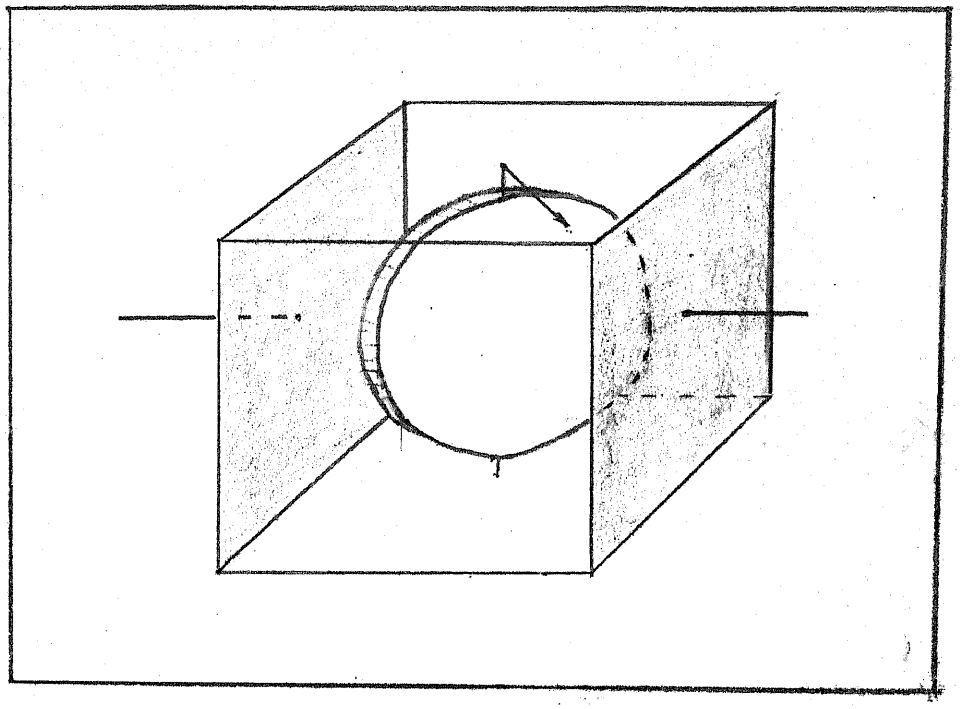

Fig. XIV. Model of Blood Cell

symmetry of the disc. The ratio of the conductance at an angle to the maximal conductance at $\theta = \frac{\pi}{2}$ is plotted on figure XV. The resultant curve can closely be represented by the formula

$$(54)\quad \frac{g(\theta)}{g_{max}} = 1 - \Delta g . \cos^2\theta$$

where Δg is the maximal relative change in conductance

$$(55)\quad \Delta g = \frac{g(\frac{\pi}{2}) - g(o)}{g(\frac{\pi}{2})} = \frac{g_{max} - g_{min}}{g_{max}}$$

In order to compute the average conductance for a random orientation of the cells a uniform probability density function P is assumed, i. e. the probability of finding the end of vector $\vec{a}$ in a certain element of area dS is directly proportional to the magnitude of dS,

$$(56)\quad P\ ds = \frac{dS}{4\pi}$$

where $\vec{a}$ is a unit vector coinciding with the axis of symmetry, and dS is an element of area of a unit sphere around the center of the disc as shown in figure XVI.

In the spherical coordinates φ and θ

$$(57)\quad dS = \sin\theta\, d\varphi\, d\theta$$

Substituting (57) into (56) gives the probability density function in the $\varphi; \theta$ plane

$$(58)\quad PdS = \frac{\sin\theta}{4\pi}\, d\varphi\, d\theta$$

In the $\varphi; \theta$ plane P is no longer uniform but sinusoidal.

The average conductance is given by:

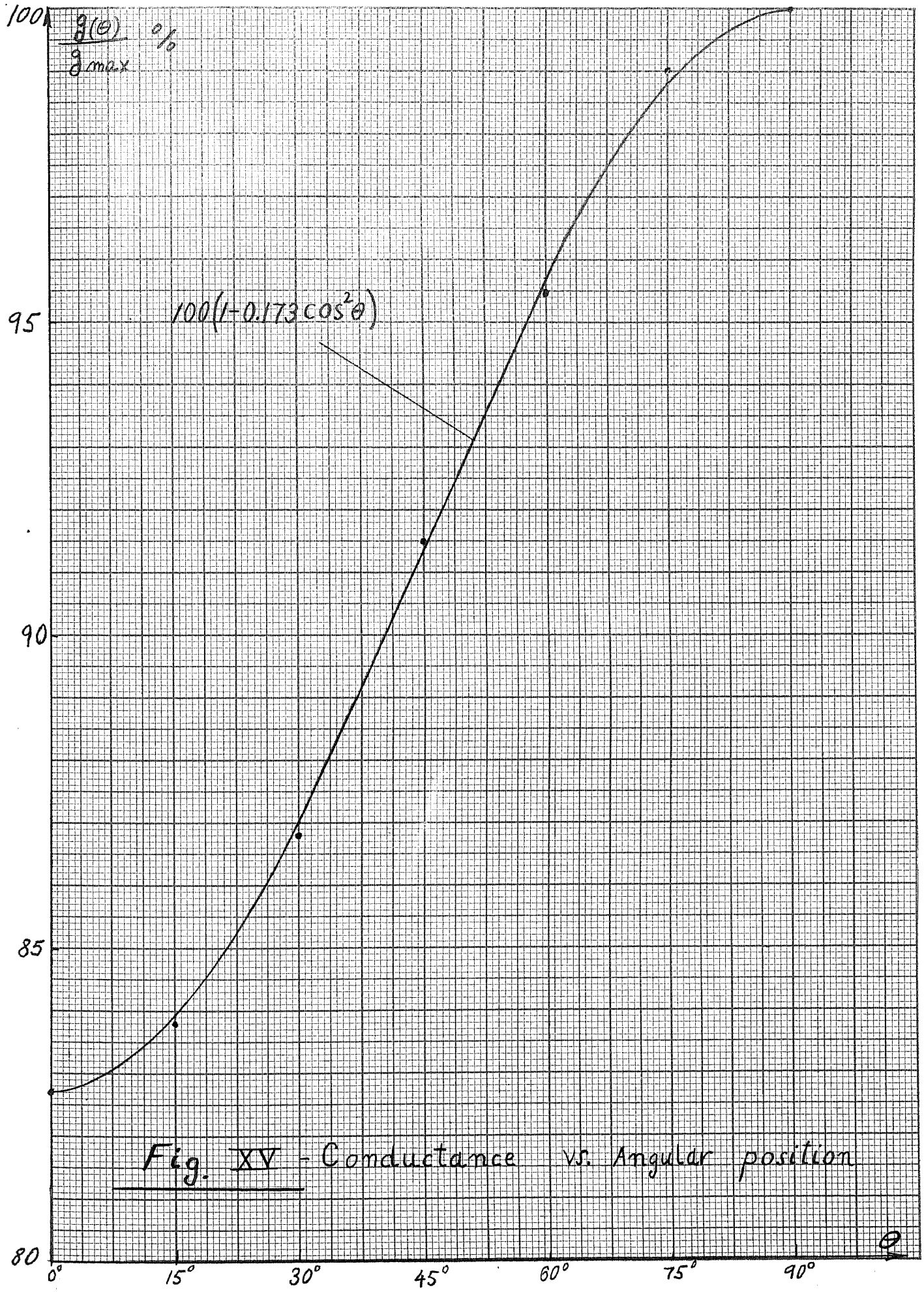

Fig. XV - Conductance vs. Angular position

TABLE NO. 5 (For Fig. XV)

Conductance Versus Angular Position of a Cell.

θ (degrees)	G (m mhos)	$\frac{G}{G_{max}}$ %	100 - 17,3 ($\omega^2 s\,\theta$)
0	0.666	82.7	82.7
15	0.675	83.8	83.9
30	0.698	86.8	87.0
45	0.738	91.5	91.35
60	0.769	95.5	95.68
75	0.797	99.0	98.82
90	0.805	100.0	100.0

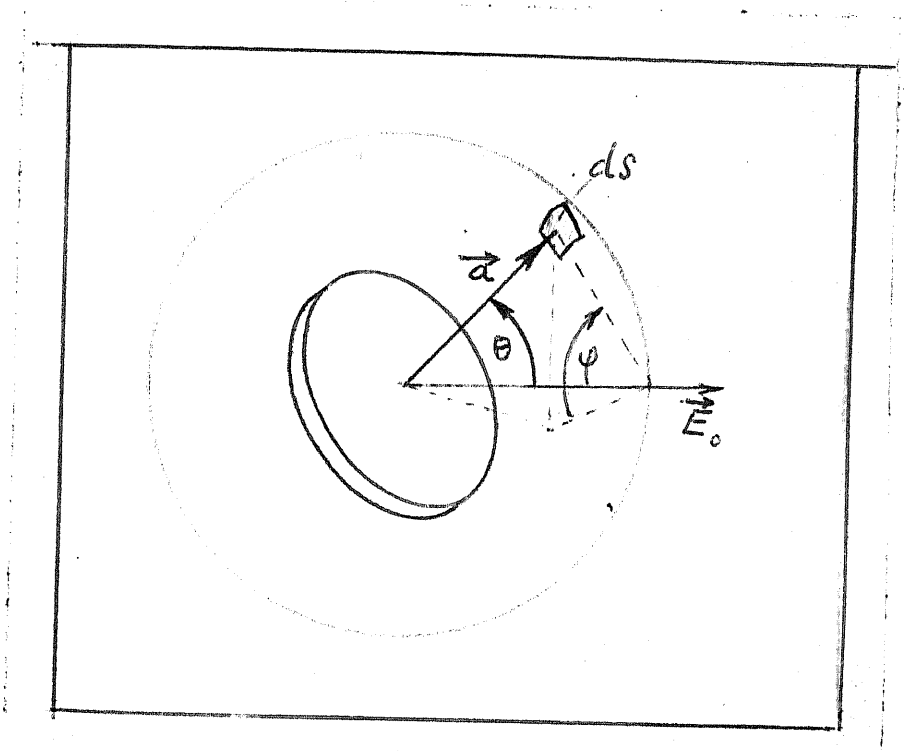

Fig. XVI . System of Coordinates

$$(59)\quad G_{av} = \iint_S g \cdot P \, dS = \frac{1}{4\pi} \int_{\varphi=0}^{2\pi} \int_{\theta=0}^{\pi} g(\theta) \sin\theta \, d\varphi \, d\theta$$

$$(60)\quad G_{av} = \int_0^{\frac{\pi}{2}} g(\theta) \sin\theta \, d\theta$$

substituting $g(\theta)$ from equation (54)

$$G_{av} = g_{max} \int_0^{\frac{\pi}{2}} (1 - \Delta g \cos^2\theta) \sin\theta \, d\theta = g_{max} \left(-\cos\theta + \Delta g \cdot \frac{1}{3} \cos^3\theta \right) \Big|_0^{\frac{\pi}{2}}$$

$$(61)\quad G_{av} = g_{max} \left(1 - \frac{\Delta g}{3}\right)$$

Substituting Δg from equation (55) gives

$$(62)\quad \frac{g_{max} - G_{av}}{g_{max}} = \frac{1}{3} \frac{g_{max} - g_{min}}{g_{max}}$$

g_{max} is also the average conductivity of blood in the extreme case of infinite rate of shear when all the blood cells present a minimal resistance to current flow, as described in Fig. XIII. However, G_{av} is the average conductivity of blood at rest, when the cells have a random distribution. Hence the maximum change in conductivity of flowing blood due only to orientation is one third of the maximum change of conductivity which was obtained in the model of Fig. XIV.

The graph of Fig. XV indicates a maximum relative change of

$$\Delta g = 17.3\%$$

We might therefore expect a maximum relative increase of 5.46% in conductivity of moving blood, with respect to its conductivity at rest. If this rate of change is added to the one computed for axial accumulation, a total maximum change of about 12% is expected which is close to the experimental result of about 10% in a steady flow.

Of course, the extreme case of complete order can never be achieved because of mutual collisions and local turbulences which occur at higher rates of flow and which upset the equilibrium position achieved in a steady laminar flow. Nevertheless, in the laminar range of flow the number of cells which obey the effects of axial accumulation and orientation, increases monotonically with the rate of flow, and hence the electrical impedance method can be used for detection of blood flow as is described in the following chapter.

CHAPTER III

EXPERIMENTAL METHODS AND DATA.

1. The Hydraulic System.

In order to evaluate and analyze the resistance changes in blood resulting from periodic velocity changes, a circulatory model was utilized incorporating the conditions of a fixed volume of blood in the segment in which the electrical impedance measurements were made.

A dual-cycle pump with a constant frequency was used to propel citrated human blood through a system of polyethylene tubes, schematicaly described in Fig. XVII. The impedance measurements were made in segments of tubing of varying diameters, ranging from 0.76 mm to 16 mm. The flow rate through the segment was varied by the use of proximally located tunnel clamps. A shunt was used in conjunction with the smaller tube segments. An electrical impedance flow meter was included in the circuit to indicate the pattern of blood flow. The volume flow per unit time was determined by collecting the blood at the outflow in a calibrated vessel.

The flowmeter, Fig. XVIII, consist of two glass tubes of 16 mm diameter, interconnected by two polyethylene tubes, A and B. The glass tube through which the blood flowed was divided into two segments by a rubber stopper having a narrow opening in it s center. The other glass tube was divided into two segments by a flexible membrane with a metal contact centrally located on the membrane. This contact was free to move towards a metal screen placed near the membrane.

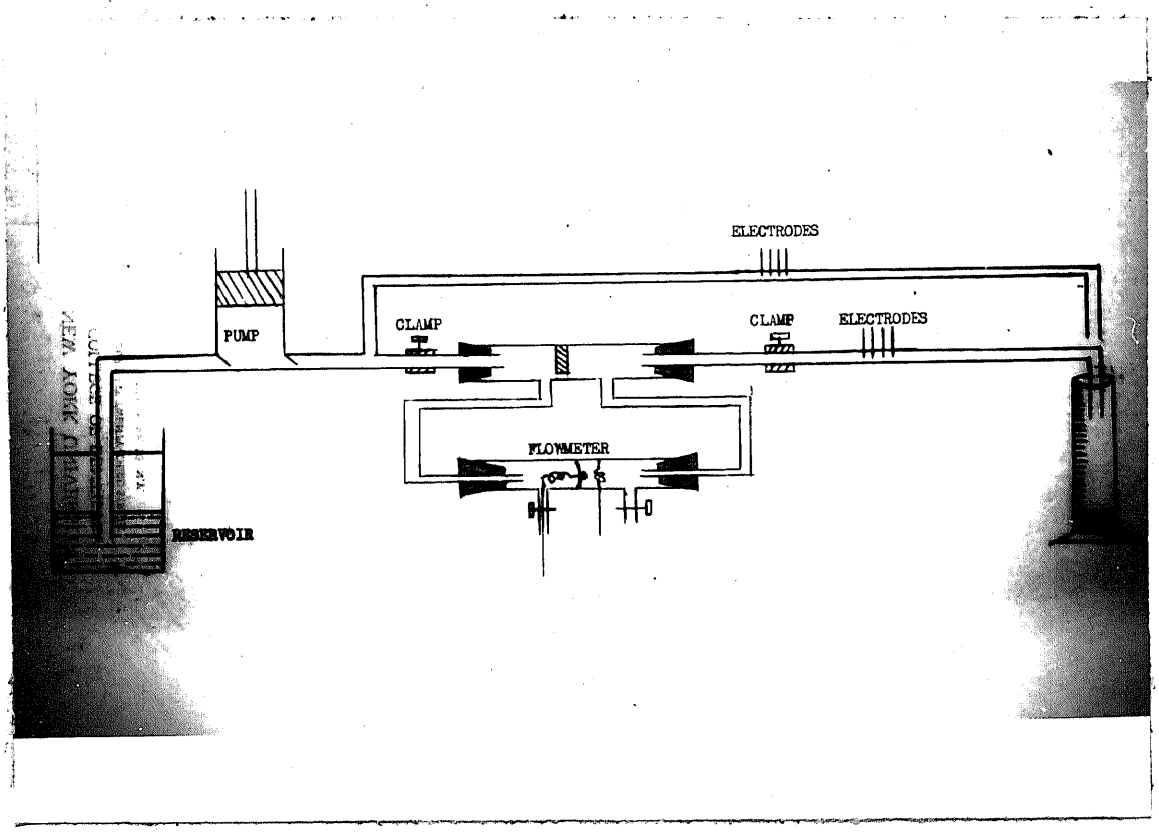

Fig. XVII The Hydraulic System

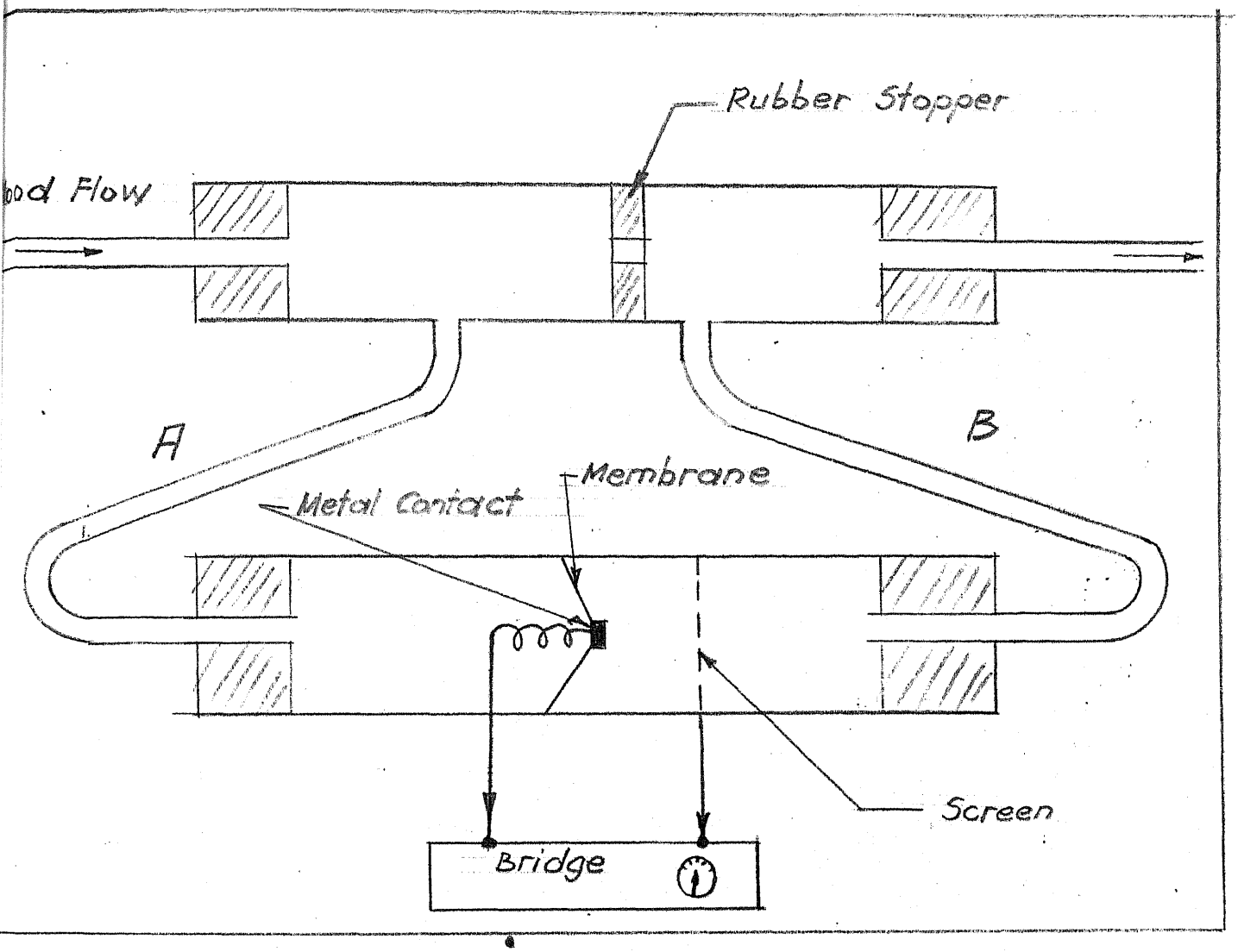

FIG. XVIII

FLOWMETER DIAGRAM

Because of the difference in diameters the velocity proximal to the rubber stopper is less than the velocity distal to the narrow opening. Therefore, the pressure in tube A is higher than the pressure in tube B. The pressure difference, $P_A - P_B$ depends on the velocity of the stream and is reflected by a decrease in the distance between the membrane and the screen. The impedance between the metal contact on the membrane and the screen will therefore decrease as the velocity increases and will unbalance an impedance bridge. The electrical signal coming from this bridge is an indication of the velocity pattern of the stream.

2. The Impedance Measurements.

a) Arrangement of Electrodes. In order to eliminate resistance changes due to a "wiping away" effect of the red blood cells from the electrodes, tetrapolar electrodes were used in conjunction with a bridge circuit resembling that of a Kelvin double bridge (see appendix I). In all the measurements the longitudinal resistance was measured by setting the electrodes along the tube in such a way that the two extreme electrodes supplied the current and the other two electrodes detected the voltage drop.

In the wide segments four hypodermic needles were inserted in the tube and used as electrodes. In the narrow tubes, cylindrical connectors were used to avoid interfering with blood flow (Fig. XIX). The distance between the current electrodes should be long enough to provide a uniform field in the middle of the segment, and the distance between the voltage electrodes can be adjusted so that the transfer

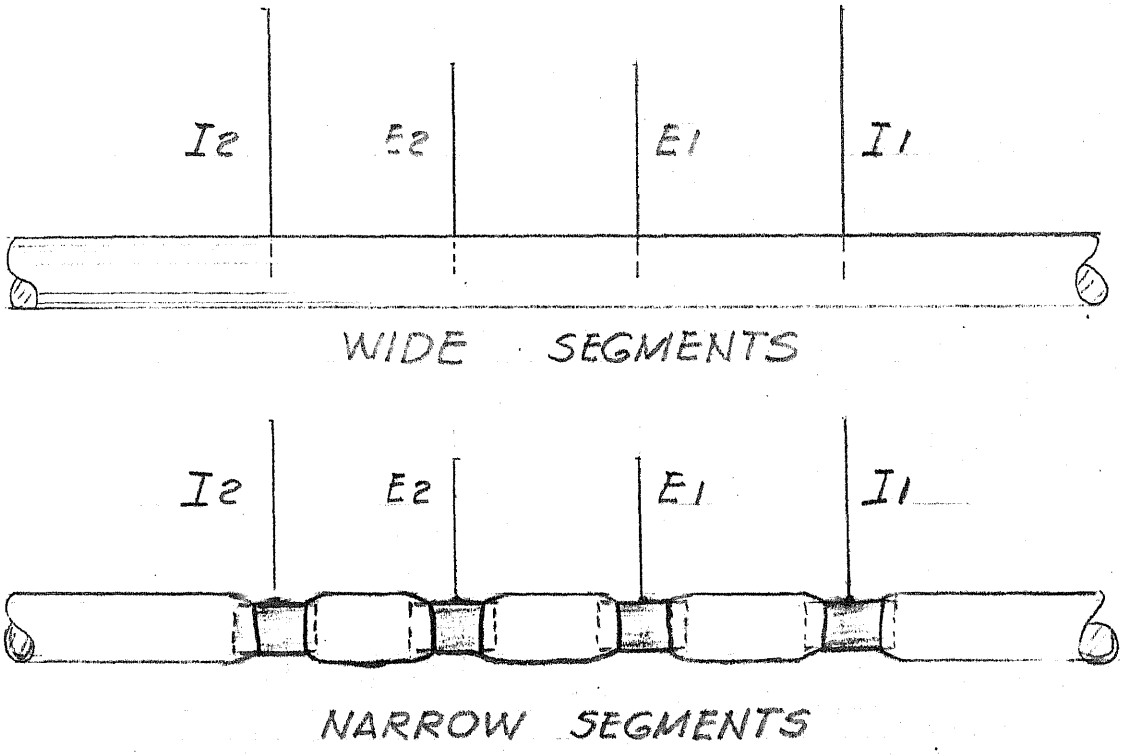

FIG. XIX . ELECTRODES ARRANGEMENT.

impedance will be within the range of measurements of the bridge.

b) The Bridge Circuit. All the impedance measurements were carried out using a transistorized device originally designed by Bagno and Liebman[13], for impedance measurements of living tissues.

The schematic of the circuit is shown in Fig. XX. Transistor Q_1 in conjunction with T_o constitutes an oscillator that generates approximately 50 kc. The output of T_o is fed to emitter follower Q_2 which isolates the oscillator from the rest of the circuit. Transformer T_1 supplies a constant voltage to the bridge circuit, consisting of R_1, R_2, R_3, the 25,000 ohm potentiometer and the blood segment. A bridge ratio of 40:1 provides a constant current in the blood segment independent of it's resistance. The voltage drop across E_1 and E_2 is counteracted by the voltage from T_2 to form a null circuit. The secondary of step-down transformer T_3 matches the input impedance of a grounded-emitter stage Q_3 while the primary presents a high impedance so that practically no current flows between points E_1 and E_2. Common-emitter amplifier Q_3 amplifies the unbalanced potential of the bridge. Impedance matching transformer T_4 couples the amplifier to a phase detector. Variable capacitor C_1 in conjunction with the core of T_o, adjusts the phase of the unbalanced bridge signal to a reference coming directly from the generator. Both signals feed the phase-sensitive detector (see appendix II). The output signal from the phase detector is directly proportional to the rhythmic changes in blood conductivity which unbalance the bridge.

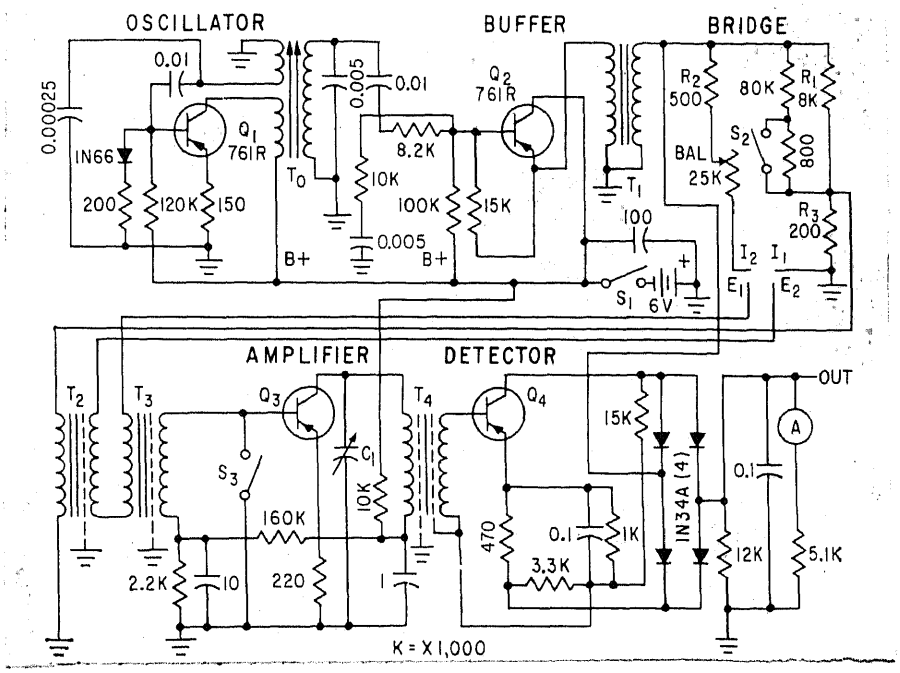

Fig. XX The Electrical Circuit of the Bridge
(After Bagno and Liebman)

The above circuit provides a signal to noise ratio of 40:1 for a resistance change of 0.1%, and has a sensitivity of 50 mv per resistance change of 1%. The instrument can be easily balanced by the 25 k potentiometer and is extremely linear.

3. Experimental Data.

The phenomena which account for the conductance changes of blood with changes in its velocity occurred with such rapidity that the impedance pulse was correlated with the velocity pulse (Fig. XXI). This was true in all the tubes employed.

When plasma or hemolyzed blood was circulated through the system the velocity pulse had no effect on impedance as shown in the lower portion of Fig. XXI.

The amplitude of the impedance pulse was directly proportional to the velocity in the entire range below saturation level. Above this level a further increase in velocity resulted in no significant change in impedance. Figures XXII, XXIII, XXIV demonstrate a gradual increase in the impedance pulses as a result of gradual increase of velocity. Fig. XXIV indicates that above saturation the wave form changes in this tube but the amplitude remains the same. The wave form change during saturation is attributed to momentary turbulance which upsets the laminar flow at the peak of the pulse.

In all of the tubes, except the largest, in which a sufficiently high velocity could not be produced, saturation occurred at a velocity of approximately 5 cm/sec (Fig. XXV).

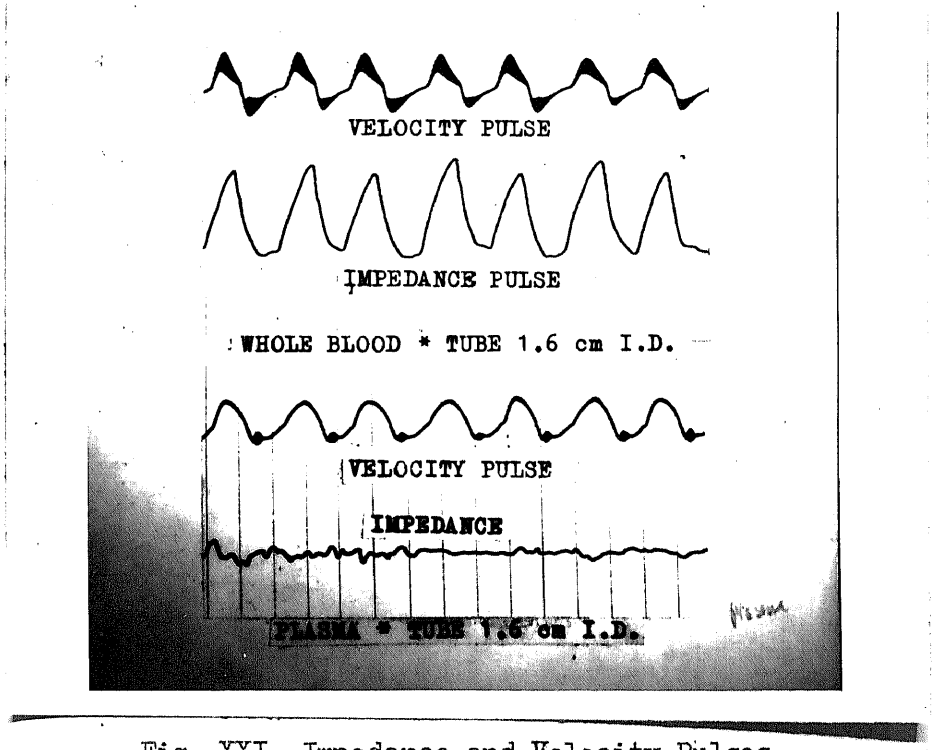

Fig. XXI Impedance and Velocity Pulses for Whole Blood and Plasma

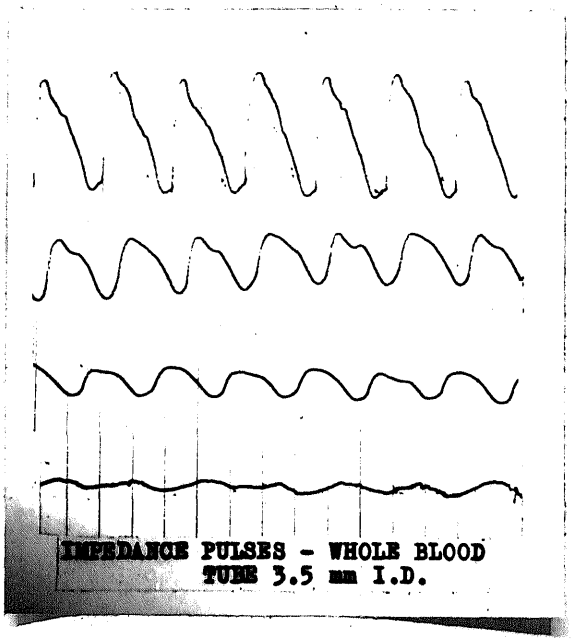

Fig. XXII

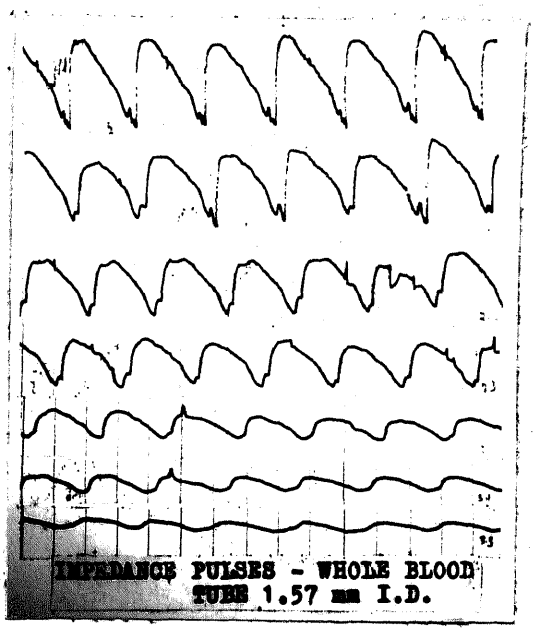

Fig. XXIII

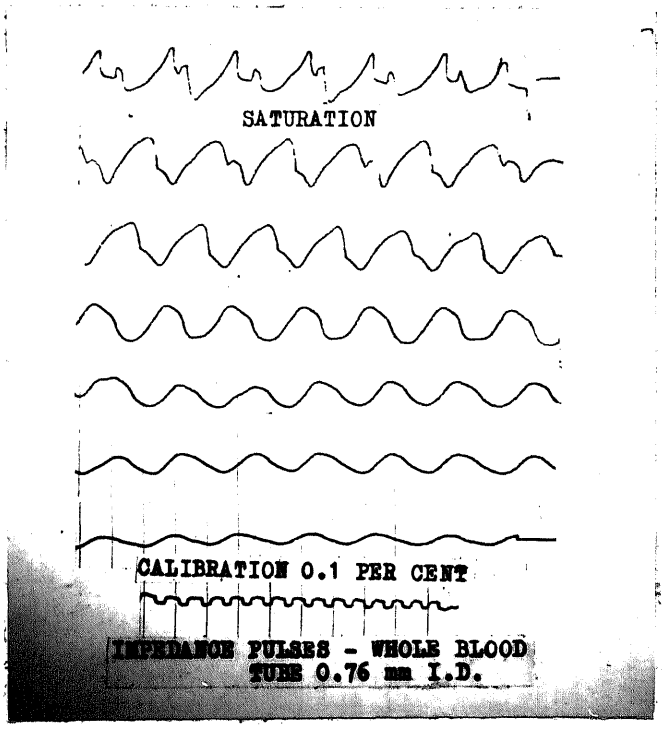

Fig. XXIV

Gradual Increase of Impedance Pulses

In Fig. XXVI the velocity is on a semi - log scale which gives a somewhat clearer picture of the variations at very low velocities.

When the impedance measurement was made after a relatively long period of steady flow, saturation occurred in the same range of velocity. However, the ultimate impedance change went as high as 10% (Fig. XXVIII) in contrast to a maximum change of approximately 2% in pulsatile flow. The difference in these results is to be attributed to the fact that a certain period of time is required for the blood cells to respond to the accumulation and orientation forces. The relative number of cells that succeed in reacting to these forces therefore depends on the time interval that the blood flows at a specific velocity.

In figures XXV, XXVI, XXVII the abscissa gives the absolute value of the relative change of impedance. The actual sign of $\frac{\Delta R}{R}$ is always negative, i.e. the impedance always decreases with velocity.

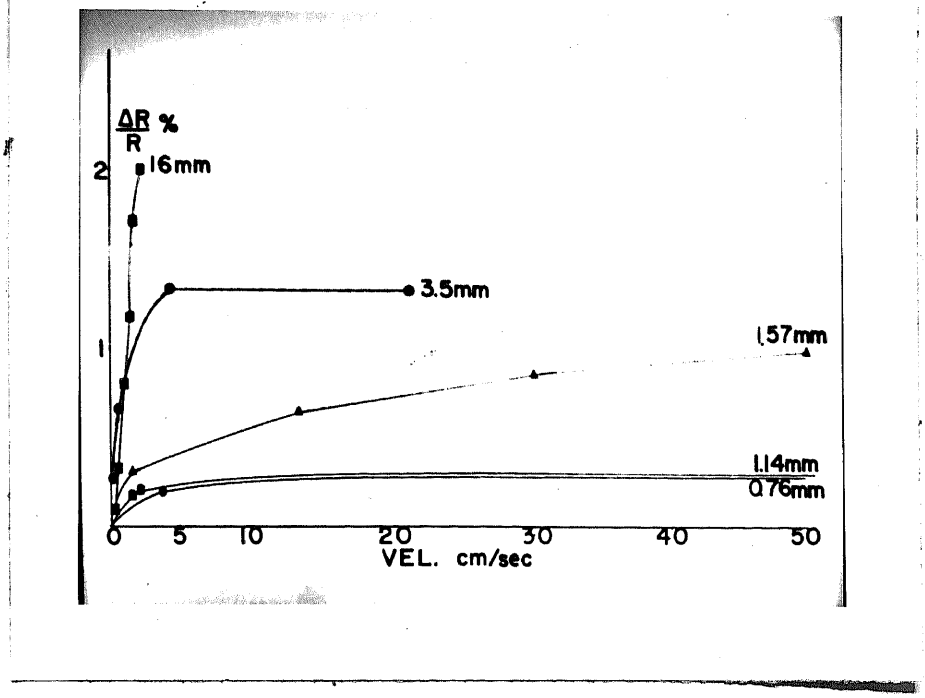

Fig. XXV

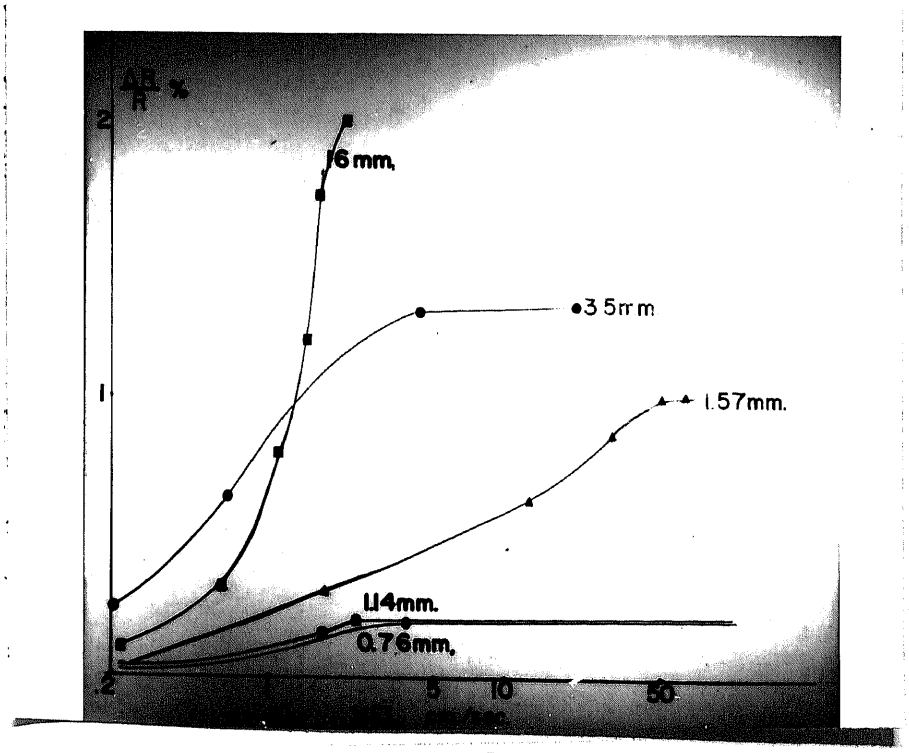

Fig. XXVI

Resistance Changes for Pulsatile Flow

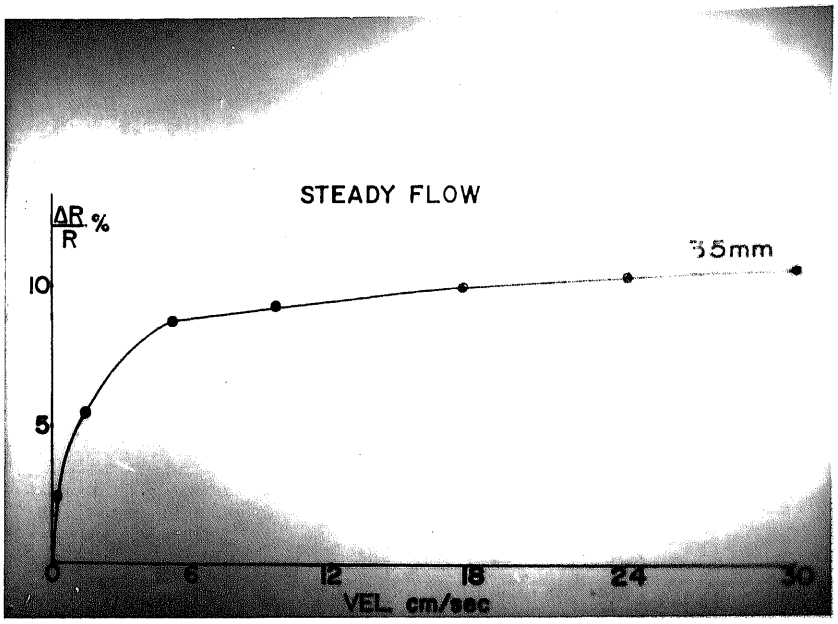

Fig. XXVII Resistance Change for Steady Flow

CONCLUSIONS

Utilization of the velocity component of blood impedance offers an extremely sensitive method for detecting changes in blood flow, at least on a qualitative level, in anatomical areas where volume changes do not occur, and especially under conditions of very low flow rates.

The instrumentation methods described in this paper provide a sensitivity of 1.5 mv per 10^{-3} c.c./sec of pulsatile flow, with a noise ration of 40:1. The electrical impedance method is the only method known to me by which we can indicate such low rates of blood flow occurring in several capillary beds of the body.

APPENDIX I

The Tetrapolar Method.

The tetrapolar method is an indirect method of impedance measurement which was developed in order to eliminate the effect of contact resistance. Instead of an entrance impedance between two terminals, a voltage transfer ratio between four terminals is measured, and it is proportional to the actual impedance.

The equivalent circuit of the system may be described as follows:

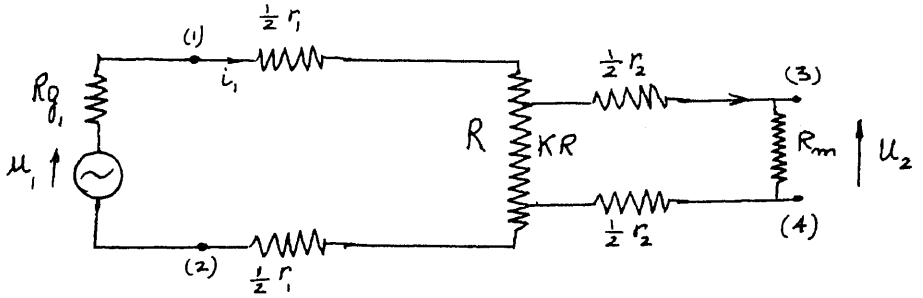

where: U_1 is a constant voltage source

Rg_1 is internal resistance of the generator

r_1 is contact resistance of terminals (1) and (2)

r_2 is contact resistance of terminals (3) and (4)

R is the measured resistance

K is potentiometer ratio

Rm is meter resistance

If the entrance resistance is measured directly between terminals (1) and (2), the result will be

$$R_{in} = R + r_1$$

the relative change in R_{in} due only to changes in the contacts resistance r_1 will be:

$$\frac{\Delta R_{in}}{R_{in}} = \frac{\Delta r_1}{R+r_1} \simeq \frac{\Delta r_1}{R}$$

The error made by this method depends therefore on the ratio between the change in contact resistance to the measured one, two parameters which are out of control.

By detecting the voltage u_2 we gain two important factors:
a) the voltage drop across r_1 is not included in the measurement,
b) by increasing Rg_1 we can make i_1 constant, independent of r_1.
The voltage drop across r_2 which at first glance seems to affect the measurement of u_2, can be also eliminated by making R_m large enough.

The voltage transfer ratio $\frac{u_2}{u_1}$ is given by

$$\frac{u_2}{u_1} = \frac{R_m \cdot R \cdot K}{(Rg_1 + r_1 + R)(r_2 + R_m) - R^2 K^2}$$

If we make $Rg_1 \gg r_1 + R$ and $R_m \gg r_2$

$\frac{u_2}{u_1} \simeq \frac{R \cdot K}{Rg_1}$ The voltage ratio becomes directly proportioned to R.

In the Bridge Circuit of Fig. XX the first condition is accomplished by a bridge ratio of 40:1. The second condition is fulfilled by a turns ratio of 8:1 in transformer T_3 which results in an impedance ratio of 64:1 between the primary and the secondary.

APPENDIX II

The Phase Detector.

The phase sensitive detector was developed in order to overcome several noise problems involved in Radar systems. It is schematically described on the following diagram.

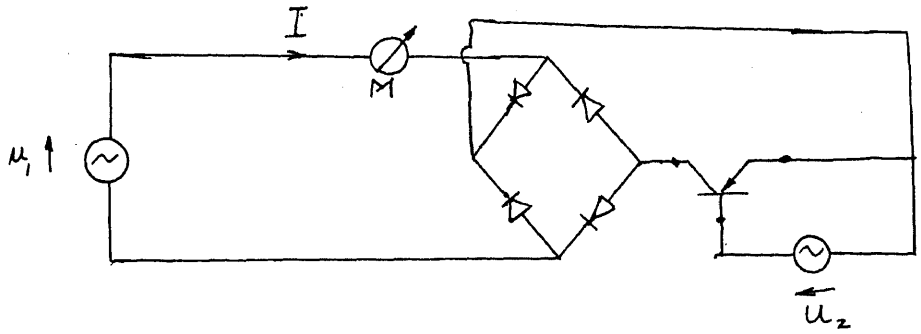

A regular Gretz bridge is driven by a constant sinusoidal voltage u_1, through a D-C ameter, M. A properly biased transistor is connected to the output of the bridge, while a sinusoidal voltage u_2 drives its base. Since the current flowing through the meter M is alternating, and M is a D-C meter, it will only respond when asymetry occurs between the positive and the negative portions of the current. No D-C current will therefore be detected if U_2 is zero. If u_2 has the same frequency and phase as u_1, the current at the negative portion will be increased while the positive will be diminished, and the meter will show a negative deflection. The contrary will happen when u_2 is 180^o out of phase with respect to u_1, a positive reading will be indicated. When u_1 and u_2 are 90^o out of phase, both positive and negative half waves will have the same shape and amplitudes and again no D-C component will be detected.

A mathematical analysis of this circuit can be carried out assuming linear relations:

$$I = u_1 G$$

where G is the conductance of the transistor. G depends upon the instantaneous voltage of the base:

$$G = G_o + A\, u_2$$

therefore: $I = u_1(G_o + A\, u_2)$

If the meter M has a long time constant, the average current is detected:

$$I_{av} = \lim_{T\to\infty} \frac{1}{T}\int_o^T u_1(G_o + A\, u_2)\, dt$$

and if $u_1 = V_1 \sin w_1 t \qquad u_2 = V_2 \sin (w_2 t + \varphi)$

$$I_{av} = \lim_{T\to\infty} \frac{1}{T}\int_o^T V_1\, V_2\, A \sin w_1 t \cdot \sin(w_2 t + \varphi)\, dt = \frac{V_1\, V_2\, A}{2} \cos\varphi\, \delta(w_1, w_2)$$

where $$\delta(i,j) = \begin{cases} 1 & i=j \\ 0 & i\neq j \end{cases}$$

The meter will only respond to signals having the same frequency as u_1, and the response will be proportional to the signal amplitude V_2 and to the cosine of the angle between the signal and u_1.

The imaginary component of the measured impedance will therefore not be detected and any noise potential not coming from the oscillator, will not affect the measurement.

REFERENCES.

1. Kümin, K., 1949, Inaug. Diss.; Freiburg i.d. Schweiz.

2. Haynes, R. H., and Burton A. C., Proceedings of the First National Biophysics Conference, New Haven, Yale University Press, 1959, p. 452.

3. Rivlin, R. S., Proceedings of the Royal Society, Vol. 193 A, 1948, p. 260.

4. Jeffery, G. B., Proceedings of the Royal Society, Vol. 102 A, 1922, p. 161.

5. Taylor, M. G., Physics in Medicine and Biology, Vol. 3 January 1959, p. 273.

6. Einstein, A., Ann. Physik, Vol. 19, 1906, p. 289.

7. Happel, J., Transactions of The New York Academy of Sciences, Vol. 20 March 1958, p. 404.

8. Pipes, L. A., Applied Mathematics for Engineers and Physicists, p. 326.

9. Maxwell, J. C., A Treatise on Electricity and Magnetism, Vol. 1, 1892, p. 440.

10. Saffman, P. G., Journal of Fluid Mechanics, Vol. 1, 1956, p. 540.

11. Fricke, H., The Physical Review, Vol. 24, November 1924, p. 575.

12. Courant, R., and Hilbert, D., Methods of Mathematical Physics, Vol. 1, p. 174.

13. Bagno, S., and Liebman, F. M., Electronics, April 10, 1959.